

From the Great Bahama Bank into the Straits of Florida: A margin architecture controlled by sea-level fluctuations and ocean currents

Flavio S. Anselmetti*
Gregor P. Eberli
Zan-Dong Ding

Comparative Sedimentology Laboratory, Rosenstiel School of Marine and Atmospheric Science, Division of Marine Geology and Geophysics, University of Miami, 4600 Rickenbacker Causeway, Miami, Florida 33149, USA

ABSTRACT

High-resolution, multichannel seismic data collected across the Great Bahama Bank margin and the adjacent Straits of Florida indicate that the deposition of Neogene–Quaternary strata in this transect are controlled by two sedimentation mechanisms: (1) west-dipping layers of the platform margin, which are a product of sea-level–controlled, platform-derived downslope sedimentation; and (2) east- or north-dipping drift deposits in the basinal areas, which are deposited by ocean currents. These two sediment systems are active simultaneously and interfinger at the toe-of-slope. The prograding system consists of sigmoidal clinoforms that advanced the margin some 25 km into the Straits of Florida. The foresets of the clinoforms are approximately 600 m high with variable slope angles that steepen significantly in the Pleistocene section. The seismic facies of the prograding clinoforms on the slope is characterized by dominant, partly chaotic, cut-and-fill geometries caused by submarine canyons that are oriented downslope. In the basin axis, seismic geometries and facies document deposition from and by currents. Most impressive is an 800-m-thick drift deposit at the confluence of the Santaren Channel and the Straits of Florida. This “Santaren Drift” is slightly asymmetric, thinning to the north. The drift displays a highly coherent seismic facies characterized by a continuous succession of reflections, indicating very regular sedimentation.

Leg 166 of the Ocean Drilling Program (ODP) drilled a transect of five deep holes between 2 and 30 km from the modern platform margin and retrieved the sediments from both

the slope and basin systems. The Neogene slope sediments consist of peri-platform oozes intercalated with turbidites, whereas the basinal drift deposits consist of more homogeneous, fine-grained carbonates that were deposited without major hiatuses by the Florida Current starting at approximately 12.4 Ma. Sea-level fluctuations, which controlled the carbonate production on Great Bahama Bank by repeated exposure of the platform top, controlled lithologic alternations and hiatuses in sedimentation across the transect. Both sedimentary systems are contained in 17 seismic sequences that were identified in the Neogene–Quaternary section. Seismic sequence boundaries were identified based on geometric unconformities beneath the Great Bahama Bank. All the sequence boundaries could be traced across the entire transect into the Straits of Florida. Biostratigraphic age determinations of seismic reflections indicate that the seismic reflections of sequence boundaries have chronostratigraphic significance across both depositional environments.

Keywords: Bahamas, carbonates, currents, drift deposits, Ocean Drilling Program, seismic stratigraphy.

INTRODUCTION

The Bahamian archipelago is a large carbonate province that is situated off the southeastern tip of the North American continent. Geologically, it is best known as a modern example of isolated carbonate platforms and deposition of shallow-water carbonates. The archipelago, however, also separates the Atlantic Ocean from the Gulf of Mexico. The Florida Current, which is a major contributor to the Gulf Stream, flows through the seaways between Florida and the Bahamas (Fig. 1). In this paper, we illustrate the platform margin-to-basin architecture of this unique depositional system, which involves both sea-level

controlled shallow-water production and current-controlled redeposition in the adjacent seaway.

Carbonate production on the platforms is controlled largely by sea-level conditions. Sediment production and off-bank transport is highest during sea-level highstands when the platform is flooded (Hine et al., 1981; Schlager, 1981; Mullins, 1983). During these times, more sediment is produced than can be accumulated on the platform top, and a large amount of sediment is transported off-bank onto the slopes (Hine et al., 1981; Glaser and Droxler, 1991; Wilber et al., 1990). Light dependency forces the carbonate-secreting organisms to maintain the depositional systems close to sea level, resulting in a nearly flat sediment surface across the entire platform. As a result, falling sea level exposes the platform and restricts sediment production to the fringes of the platform. With renewed flooding of the platform, sediment production and off-bank transport resumes, depositing a “highstand” wedge on the leeward slope of the western Great Bahama Bank (Wilber et al., 1990). During most of the Neogene, the Great Bahama Bank was a ramp-like platform that only evolved into the steep-sided modern platform during the late Pliocene (Eberli and Ginsburg, 1987, 1989; Eberli et al., 1997b). In a ramp-like system, a sea-level lowering results in a basinward shift in facies distribution rather than in a dramatic halt of carbonate sedimentation. For example, lower Pliocene sediments of borehole Clino (Bahamas Drilling Project; Fig. 1), which were deposited on a distally steepened ramp, have a rather uniform composition, and differentiation of highstand and lowstand packages is more difficult (Westphal, 1998). However, in both cases, the sea-level controlled sedimentation produced pulses of progradation in the adjacent seaways (Eberli and Ginsburg, 1989; Wilber et al., 1990). A grid of industry seismic data collected over the northwestern corner of Great Bahama Bank revealed for the first time a complicated, internal architecture of the

*Present address: Geologisches Institut, Swiss Federal Institute of Technology ETHZ, Sonneggstrasse 5, CH-8092 Zürich, Switzerland; e-mail: flavio@erdw.ethz.ch.

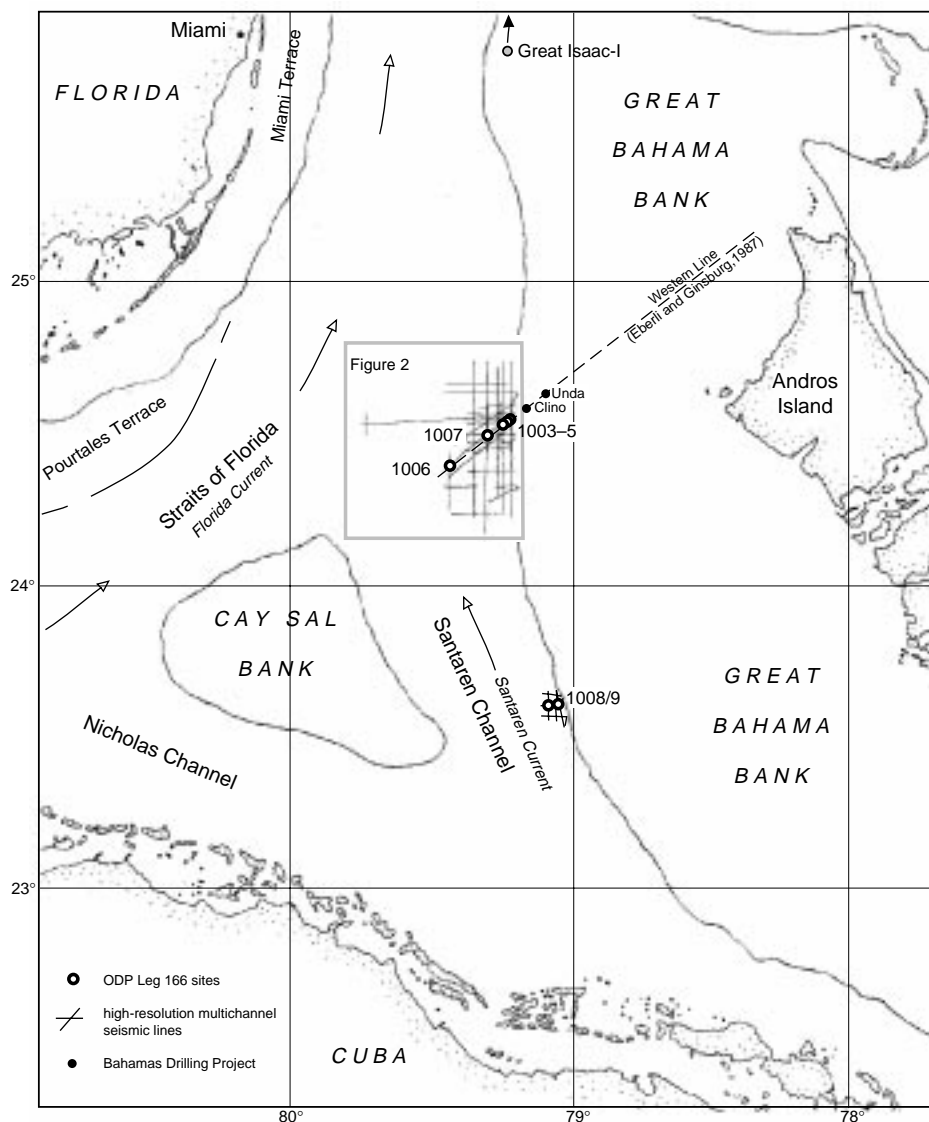


Figure 1. Regional map, showing location of carbonate platforms and deep-water straits. Major ocean currents are indicated with arrows. Unda and Clino are two drill holes of the Bahamas Drilling Project positioned on Great Bahama Bank along the Western Geophysical line. The box represents area of Figure 2 with seismic sections and Ocean Drilling Program Leg 166 drill sites. Great Isaac-I is an industrial drill site at the northwestern corner of Great Bahama Bank just outside the displayed area (as indicated by dark arrow).

bank, which once consisted of three smaller platforms that became welded together by basinal infilling and progradational processes (Eberli and Ginsburg, 1987).

The Bahamian archipelago, together with Florida and the Greater Antilles, separates the Atlantic Ocean from the Gulf of Mexico and the Caribbean. The connection between these oceans is limited to the seaways between these three landmasses. As such, the seaways act as a “valve” for the Florida Current that flows between Florida and the Bahamas into the North Atlantic, where it converges with the smaller Antilles Current to form the Gulf Stream. The Florida Current

is a strong surface current, producing erosion and hiatuses on the Miami Terrace and deposition of thick drift deposits in the deeper portions and in the lee of the current (Mullins and Neumann, 1979; Mullins et al., 1980; Brunner, 1984a, 1984b). The long-term current strength is primarily controlled by paleotectonic and climatic factors (Kaneps, 1979; Mullins and Neumann, 1979; Pinet and Popenoe, 1985). Short-term sea-level falls intensify the currents in the seaways because of restriction of the channel area (Richardson et al., 1969).

A large number of seismic data sets and coring expeditions in the seaways has revealed the

general anatomy of the slopes and basins (Schlager et al., 1976; Mullins and Neumann, 1979; Schlager and Chermak, 1979; Crevello and Schlager, 1980; Sheridan et al., 1981; Mullins et al., 1984, 1987; Ladd and Sheridan, 1987). Ocean Drilling Program (ODP) Leg 101 drilled these slopes and documented their platform progradation, facies, and sedimentation processes (Austin et al., 1988; Harwood and Towers, 1988; Schlager et al., 1988).

The purpose of this paper is to document through high-resolution seismic data how the sea-level-controlled, prograding-slope carbonates interfinger with current deposits in the more distal portions of the Straits of Florida to construct the margin and basin architecture. Furthermore, we document that the depositional surfaces are imaged as seismic reflections and that the seismic-reflection data provide an accurate picture of the platform and basin geometries. The influence of sea level is most pronounced in the prograding portion of Great Bahama Bank, where laterally stacked sequences provide a high-resolution record of Neogene and Quaternary sea-level fluctuations (Eberli and Ginsburg, 1987, 1989; Eberli et al., 1997a). Current control is dominant in the basinal portion of a transect, where a thick sediment drift accumulates. On the lower slope, drift deposits interfinger with the prograding slope deposits within the same depositional sequence. A high-resolution, multichannel seismic-data set acquired in the spring of 1994 reveals the anatomy of this dual system in great detail. Cores from five drill sites of ODP Leg 166 within the study area provide the sedimentologic calibration of the seismic data.

METHODS

To image the anatomy of the western margin of Great Bahama Bank, approximately 1000 km of multichannel seismic lines were acquired in June 1994 onboard the R/V *Lone Star*, operated by Rice University, Houston, Texas (Figs. 1 and 2). The sections were shot using a 45/105 in³ GI airgun (710 and 1530 cm³) operated at 2200 psi (1.5 MPa) and 2 m water depth. A 600-m-long, 24-channel streamer received the signals in a water depth of 3–4 m. Navigation of seismic tracks was obtained through a global positioning system (GPS). Seismic data were recorded and stored with the ELICS system and processed at the seismic laboratory of the University of Miami with the ITA processing package. The acoustic signal of the GI airgun is characterized by a frequency spectra between 20 and 500 Hz, with a central frequency of approximately 100–200 Hz. For data processing, a time-variable highpass filter was applied, ranging from 40–50 Hz in the shallow parts to 20–30 Hz in the

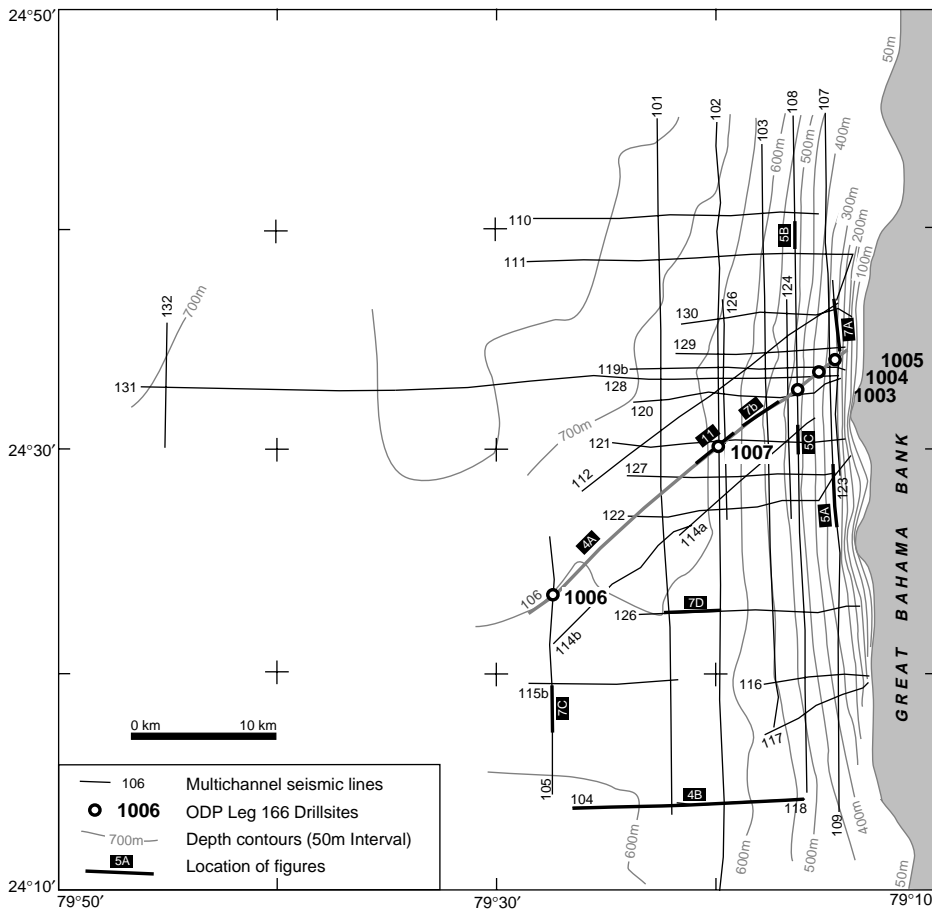


Figure 2. Base map of high-resolution, multichannel seismic sections with locations of Ocean Drilling Program Leg 166 drill sites (1003–1007) and water depth contours with 50 m intervals. Depth contours were interpolated using seismic data for the Santaren Channel and navigation chart for the bank margin. The locations of displayed seismic sections (Figs. 4, 5, 7, and 11) are indicated with bold tracks and numbers in black boxes.

deeper zones, whereas the lowpass filter was set throughout to 450–500 Hz. Due to the sharp amplitude peak of the GI airgun, which is hardly disturbed by a bubble pulse, the seismic resolution can reach 5 m, particularly in the low-velocity drift deposits that show a highly coherent seismic facies. After common depth point (CDP) stacking (12-fold), migrating, and filtering, an automatic gain control (AGC) was applied for the display of all sections with a window length of 100 ms. Finally, a Landmark 2D program was used for interpretation of the processed seismic sections. Seismic horizons could be traced throughout the grid to construct isopach maps of various units.

The displayed seismic lines are all plotted in an amplitude-coded fashion, so that black represents the positive and gray the negative polarity signals. For gray-scale figures, the blue color tone appears black, and the red appears gray. Because the first pulse of the airgun signal is a neg-

ative excursion, the sea floor and all layers with a downward increasing acoustic impedance are characterized by a red (gray) first reflection. The reference position of the sea floor and all seismic horizons is thus defined and picked in the center of the first negative peak. The burial depth in two-way time is the measured peak-to-peak distance between the negative wiggles of sea floor and the center of the picked subsurface reflection.

The seismic data served as a site survey for the “Bahamas transect,” ODP Leg 166. In spring 1996, ODP Leg 166 drilled at five sites (Sites 1003–1007) along the transect seismic line 106 at the cross sections of intersecting lines (Eberli et al., 1997a). Average core recovery was about 55%. All sites were logged with a full suite of wireline tools. A checkshot survey using a 120 in³ (1966 cm³) airgun was performed at the four deepest sites, which proved to be extremely valuable, because neither the integrated sonic log nor the shipboard velocity measurements pro-

vided an accurate velocity profile (Eberli et al., 1997a). The first arrivals of the checkshots signals allow for a precise two-way traveltime-to-depth conversion, so that the drilled lithologies can be correlated with high accuracy to the high-resolution seismic sections. Figure 3 displays the subbottom two-way traveltime vs. depth curve for all investigated sites. Because the seismic sections were not depth migrated, these curves can be used to calculate the depth-of-reflection events seen on the displayed sections.

Standard ODP operations on shipboard core included sedimentologic, biostratigraphic, paleomagnetic, and geochemical analyses (Eberli et al., 1997a). Ages for nanofossil and planktonic foraminiferal events used during ODP Leg 166 were based mainly on the geomagnetic polarity time scale (GPTS) of Berggren et al. (1995). The ages of epoch boundaries were taken from the above-mentioned timescale, except for the Miocene-Pliocene boundary, for which we used 5.6 Ma. In the core, the Miocene-Pliocene boundary was recognized as the top of the range of the calcareous nanofossil *Discoaster quinqueramus* (Eberli et al., 1997a).

SEISMIC DATA DESCRIPTION: SEISMIC FACIES AND GEOMETRIES

The geometry of the seismic reflections indicates two major depositional systems that together form the slope-to-basin transition west of the modern platform margin of Great Bahama Bank (Fig. 4). The first system consists of west-dipping layers in the platform-proximal areas and documents downslope deposition on the bank slope. These sediments interfinger at the toe-of-slope with the second major system, which consists of horizontal or east-to-northeast-dipping current deposits that wedge out towards the platform. These two types of deposits, indicating two sediment transport directions, compose the architecture of the slope-to-basin transition.

Slope Facies (West-Dipping Layers)

The prograding system on the western slope of Great Bahama Bank consists of sigmoidal clinoforms that have advanced the margin some 25 km into the Straits of Florida (Eberli and Ginsburg, 1987, 1989). The west-dipping slope deposits are characterized by foresets of clinoforms that are approximately 600 m in height and that steepen significantly in the Pleistocene section (slope angles up to 9°). The clinoform packages thin basinward and display a variety of seismic facies. On dip lines, the inclined reflections are variable in amplitude and continuity. In the middle- and lower-slope sections, continuity of seismic reflections is short, resulting in a nearly chaotic

seismic facies. At the toe-of-slope and farther basinward, continuity of the reflections increases (Fig. 4). The reflection amplitude of the slope sections also varies. Discontinuous high-amplitude packages are interrupted by a low-amplitude, nearly transparent unit of about 100 ms equivalent thickness that forms the early Pliocene slope (Figs. 4 and 5, A and C).

On strike sections, the entire upper and middle portions of the slope are dissected by channels of variable size (Fig. 5), which occur at different stratigraphic levels. Many of the channelized sections display a persistent cut-and-fill geometry (Fig. 5) that can be recognized throughout the entire Neogene depositional succession. These numerous canyon-like erosional features result in truncated and noncoherent seismic reflections. Several horizons and units exhibit a greater number of these canyons. In particular, the lower Pliocene section, which appears seismically almost transparent, shows the most spectacular incisions with relief in excess of 100 m (Fig. 5A). A three-dimensional-perspective plot in two-way travelt ime of the seismic horizon forming these late Pliocene canyons clearly shows numerous canyons that originate upslope close to the platform edge (Fig. 6). They are oriented towards the west, suggesting that the erosive current forming these canyons was oriented downslope. At the base of slope, however, all of these canyons feed a slope-parallel depression that was filled with drift sediments during the late Pliocene.

Although the early-late Pliocene boundary marks the most prominent period of channeling, many other Neogene horizons are also characterized by canyon-like incisions. These canyons are occasionally arranged in a complicated stacking pattern, resulting from lateral migration through time (Fig. 5B). Other examples (Fig. 5C) show that these canyons can also remain stable at one slope position and thus simply stack vertically. Even in sections in which major canyons are absent, the seismic facies of the slope deposits is characterized by frequent smaller-scale incisions, yielding incoherent and irregular seismic-reflection patterns (Fig. 7, A and B). All these observations document the combined effect of erosional and depositional processes that influenced the geometry and facies of these slope sediments.

Basinal Facies (Horizontal to East-Northeast-Dipping Layers)

Very continuous seismic reflections, dipping towards the northeast (thus towards the platform margin), indicate sediments that accumulated in the basin axis rather than on the slope. In contrast to the westward-directed downslope transport

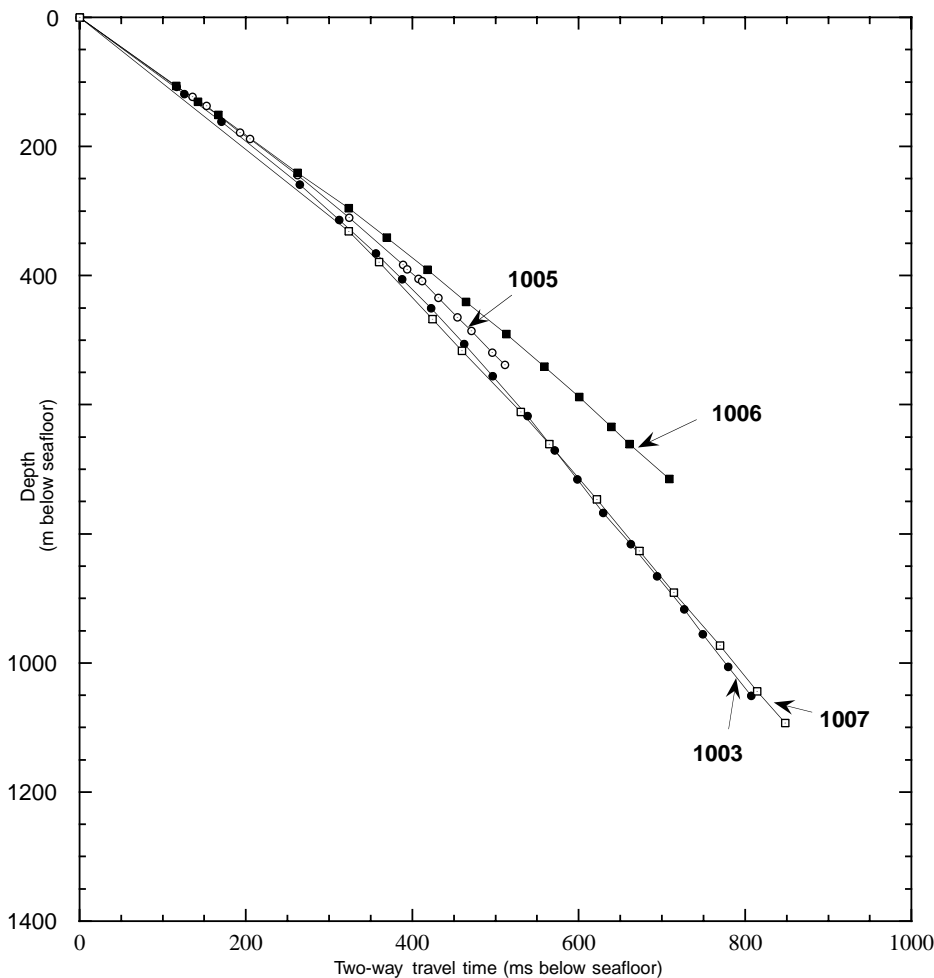


Figure 3. Two-way traveltime (TWTT) to depth conversion based on checkshot experiments conducted at drillsites of Ocean Drilling Program Leg 166, reflecting the distribution of acoustic velocity along the transect. Checkshot surveys were performed with a 120 in³ airgun (1966 cm³) at four sites, resulting in a time-depth curve for each site (Eberli et al., 1997a). Note the lateral variability in downhole velocity distribution.

that moves sediment from the platform top into the Straits of Florida-Santaren Channel, the high lateral consistency, north-northeast-oriented downlap surfaces, and sand-wave geometries indicate that accumulation of these basinal deposits was controlled by currents.

On our seismic data, three types of seismic facies indicate current deposition and erosion. (1) Large-scale sediment drifts are characterized by highly continuous, low-amplitude seismic reflections forming an elongated sediment package in the channel axis up to 1000 m thick. Figure 4A shows how the drift package wedges out towards the platform along the central seismic line 106. Farther south, along lines 104 and 118 (Fig. 4B), the drift deposit becomes even thicker because, between the two displayed sections (Fig. 4, A and B), some reflections within the

drift package downlap and terminate towards the north, indicating a current pattern that flowed generally northward. (2) In some sections, regularly spaced, north-northeast-prograding, wavy low-amplitude reflections occur within thin stratigraphic horizons (Fig. 7C). (3) In a few cases, the current activity is manifest as erosional features, which are best recognized on the flanks of the drift mounds, where the continuous mound reflections are truncated by wide and shallow depressions that subsequently were filled with sediment that forms similar continuous reflections.

The transition between slope and drift deposits can be gradual, as seen in the Miocene sections, where the slope angle decreases slowly towards the Straits of Florida and where the slope package changes into horizontally layered drift

geometries (Fig. 4). The Pliocene sections, in contrast, are characterized by more pronounced interfingering of the two depositional systems. Packages of lobe-shaped drift deposits partly downlap and onlap onto lower-slope sediments along distinct surfaces.

Deep-Water Mounds

The smooth reflection of the sediment-water interface is interrupted by isolated mounds in the lower portion of the slope and the basinal deposits below water depths of approximately 450 m

(Figs. 4B and 7D). The heights of these mounds vary and range from values that are barely visible on the seismic sections—i.e., <5–10 m—to heights of nearly 50 meters. The widths of the mounds are also variable and reach a maximum of a few hundred meters (Fig. 7D has a vertical exaggeration of 15×). Their internal character is mostly chaotic to discontinuous. A velocity pull-up below each of these mounds indicates a relatively high internal velocity.

INTERPRETATION AND CORRELATION WITH PHYSICAL PROPERTIES

The cores from ODP Sites 1003–1007 provided the ground truth measurements for the seismic facies and the geometries of the platform-basin transect along the western Great Bahama Bank (Fig. 1 and Table 1; Eberli et al., 1997a). The slope deposits drilled and recovered at these sites consist of alternations of partly unconsolidated peri-platform oozes with interbedded calcareous turbidites. Sedimentation rates on the slope are highly variable; several hardgrounds document periods of nondeposition (Eberli et al., 1997a). This pattern reflects the cyclic sedimentation input as a result of repeated flooding and exposure of the platform top. The turbidites are most abundant at Site 1007, where the depositional environment is closer to the toe-of-slope, indicating a turbidite bypass at Sites 1003–1005 higher up on the slope. This sedimentation pattern is recorded in the seismic facies and the geometries of the reflections. Because differential diagenesis results in strong impedance contrast between turbidites and peri-platform oozes (Eberli, 1988), seismic reflectivity of the slope deposits is high, resulting in a high-amplitude, but low-coherent, seismic facies. Figure 8 displays the sonic log of Site 1003 on the slope. This log clearly documents the small-scale, thin-bedded alternations of layers with higher and lower sonic velocities. Only the section between 160 and 230 m below sea floor (mbsf) appears very homogeneous on the logs (Fig. 8) and shows very low acoustic properties over the entire interval. These lower Pliocene carbonates are only semi-indurated and have an almost transparent seismic facies (Fig. 5A), which can be recognized in the entire investigated slope section (see slope sediments above the Miocene-Pliocene boundary on Fig. 4). This seismically transparent and largely unconsolidated interval of the lower Pliocene slope deposits is obviously prone to incisions by downslope currents that commonly nucleate submarine canyons (Figs. 5 and 6). The positions of these canyons on the lower and upper slope, lying up to several hundred meters below the paleo-platform margin, clearly indicate that these erosional features are of submarine origin. Although

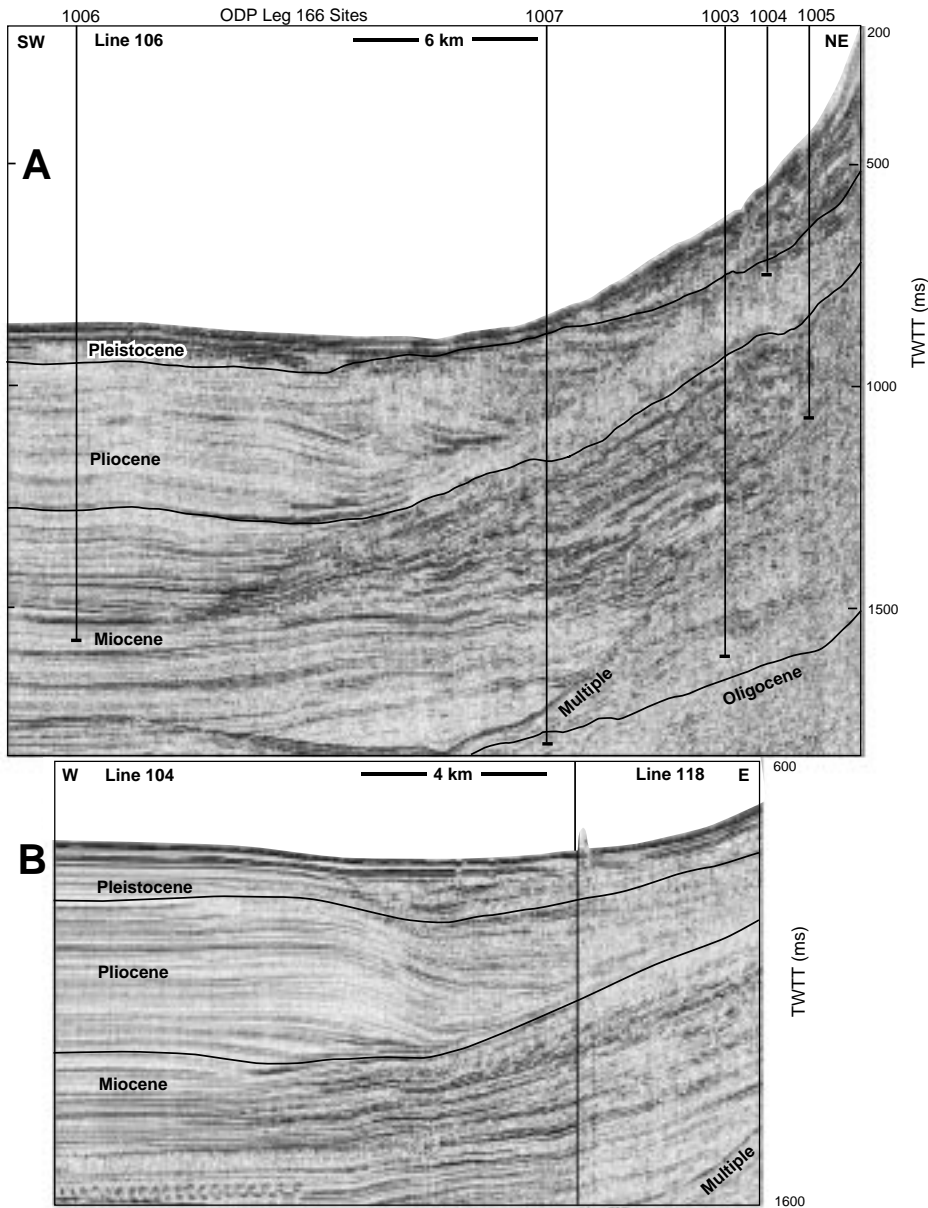


Figure 4. Seismic dip sections (vertical exaggeration ~10×). See Figure 2 for locations. (A) Line 106 is located at the center of the survey. (B) Lines 104/118 are located at the southern end of the survey. Line 106 was projected parallel to the platform; because it runs oblique to the modern platform margin, it was squeezed horizontally to match the scale of the southern dip lines. Both transects show the sedimentary geometries of two major depositional systems. Westward dipping reflections in the proximal zones document deposition on the slope of peri-platform oozes and turbidites, whereas horizontal and eastward dipping reflections in the basinal parts originate from drift deposits underneath the Straits of Florida. Both systems interfinger at the toe-of-slope.

channeling is a common phenomenon on the slope, concentrated deep incisions along several stratigraphic horizons indicate that some events were more strongly erosional than others. For example, major incisions around the early-late Pliocene boundary document that this time must have been one of major downslope erosion (Figs. 5 and 6). This slope erosion follows an early Pliocene pulse of very homogenous periplatform deposition (Eberli et al., 1997a). Incision started at approximately 3.6 Ma and continued up to about 3.1 Ma, and, therefore, slightly predates the onset of Northern Hemisphere glaciation (Raymo et al., 1992).

The large mound in the basinal section is interpreted as a large drift deposit because the seismic character and the geometries of this deposit display all the classic seismic features of drifts (McCave and Tucholke, 1986). These features include the following: (1) sediment thickness exceeds that of the adjacent sediment cover, (2) the internal reflections are weak but laterally very continuous, (3) this sediment package is underlain by undulating reflections that indicate earlier development of sediment waves, and (4) the deposit thickens axially and thins laterally. With its internal, continuous, low-amplitude reflections, this mound is similar to hemiconical bodies at the corners of both Little and Great Bahama Banks that were interpreted as drift deposits by Mullins et al. (1980). Because of its position at the confluence of the Santaren Channel and the Straits of Florida, we call this unit the "Santaren Drift."

The thin, discontinuous wavy seismic facies within the drift (Fig. 7C) is interpreted as migrating sediment waves produced by currents that were strong enough to cause bedload traction (Jordan et al., 1964; Mountain and Tucholke, 1989). A variation of this type of deposit was reported by Denny et al. (1994) in the western Straits of Florida, where small mounds are either related to variable erosion of surrounding strata by bottom currents or to levee deposits of erosional channels. Erosion in the axis of the seaways might be caused by eddies and/or by the Florida Current touching the bottom of the Straits of Florida during relative sea-level lowstands (Richardson et al., 1969).

At Site 1006, 717.3 m of the Santaren Drift were recovered; drilling penetrated through the upper Miocene–Holocene package of drift deposits in the most distal position of the seismic line 106. The cores consist of alternations of nanofossil oozes and hemipelagic carbonates with a variable amount of clay minerals. Biostratigraphic dating shows that deposition was almost continuous and, unlike that on the slope, recorded the paleoenvironmental evolution without major hiatus. Because drift deposition is mainly an in-

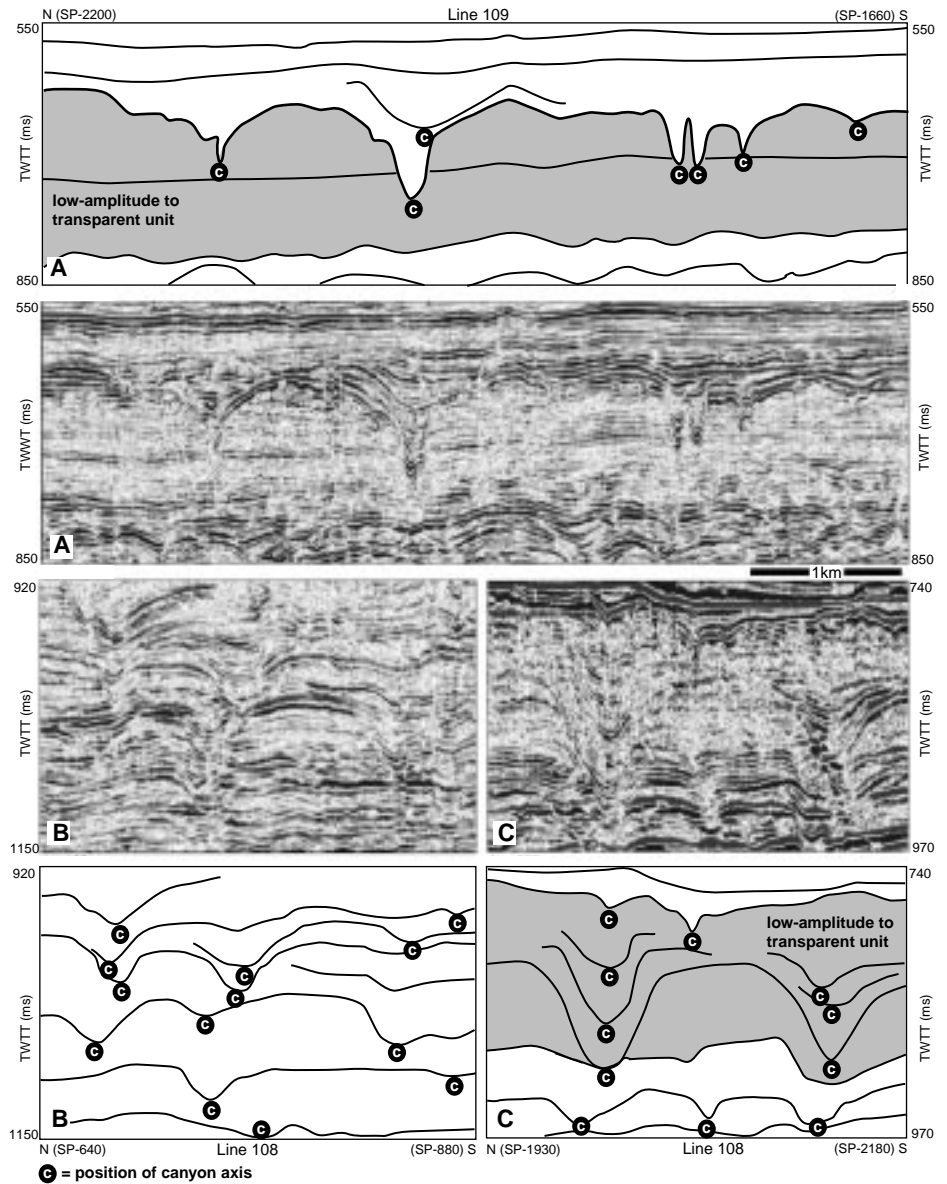


Figure 5. Seismic images (vertical exaggeration ~10×) with line drawings showing submarine canyons that have incised the slope sediments of seismic sequence *f*. (A) Seismic section shows the major phase of incision at the early-to-late Pliocene boundary. Deep canyons incise the early Pliocene sediments, which are unconsolidated and thus seismically almost transparent. (B) This seismic section shows that the early Pliocene events are characterized by several phases of submarine erosion. The channels moved laterally through time, resulting in a complicated lateral and vertical stacking pattern. (C) This section documents two canyons that only display a vertical stacking and no lateral shifts. Interpretation of seismic sections shown in B and C are shown below respective figures.

stantaneous redeposition of sediments rather than a reworking of former strata, the stratigraphic order in the drift sediments is maintained (Eberli et al., 1997a). Thickening of the packages between the basinal reflections, which is interpreted as the onset of the drift deposit, started at approximately 12.4 Ma. This age coincides with the intensification of the loop current in the Gulf of Mexico and also with the onset of the North At-

lantic deep water (NADW) circulation (Mullins et al., 1987; Wright and Miller, 1993). This timing suggests that the Florida Current acted as the shallow limb of the Atlantic conveyor from that time to the present.

The prominent, mounded, bathymetric features on the sediment drifts and atop the lower slope (Fig. 7D) are interpreted as deep-water coral reefs. Mullins and Neumann (1979) encountered

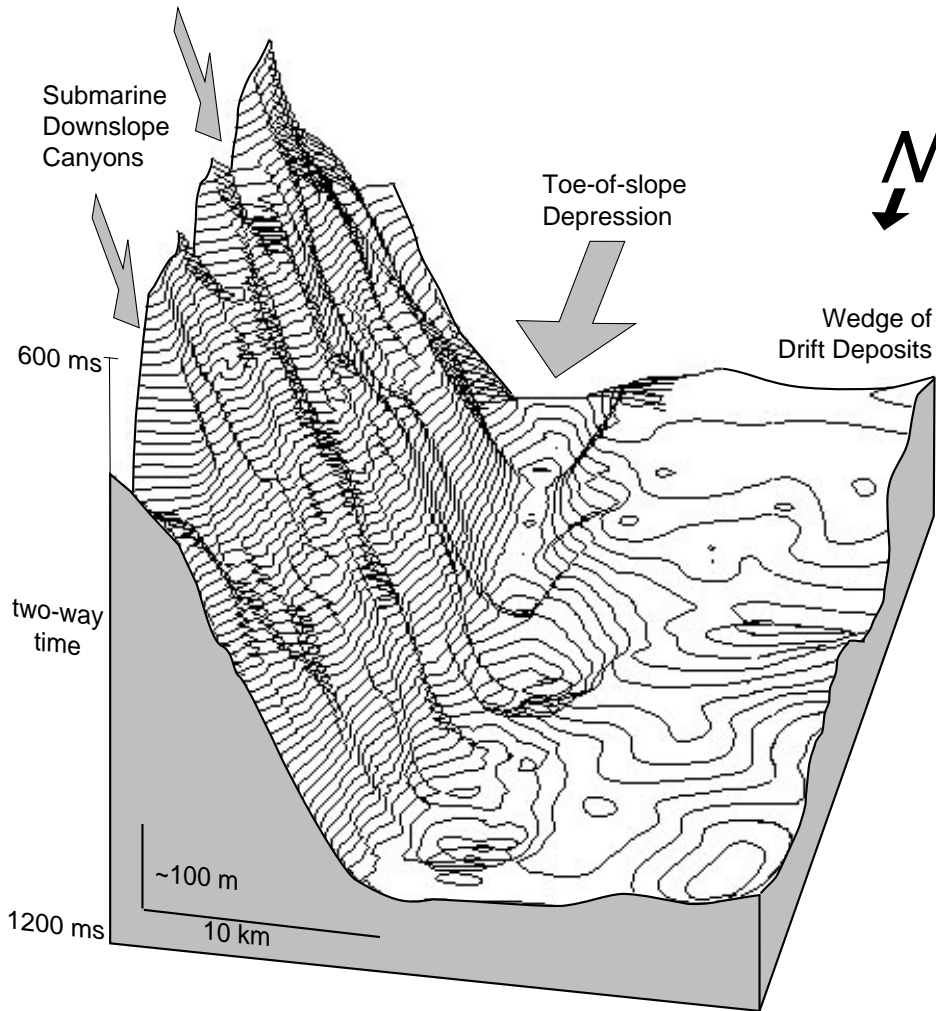


Figure 6. Vertically exaggerated (200 \times), three-dimensional view (in two-way traveltime) of seismic sequence boundary E, documenting sea-floor topography at the end of the early Pliocene. Multiple submarine canyons incise the platform flank and are oriented downslope, where they merge into a margin-parallel depression at the toe-of-slope. This geometry suggests that the canyons result from erosion by downslope transport and not from erosion by margin-parallel ocean currents. The erosional process, however, is not well understood, because no breccias or major coarse-grained units infill the canyons. The shallowing towards the west in the Santaren Channel–Straits of Florida is a result of a thick wedge of drift deposits that were transported and redeposited by ocean currents.

similar features on the hemiconical drift deposit at the northwest corner of Great Bahama Bank and called them lithohermes. Submersible diving and sampling revealed that these mounds are ahermatypic coral edifices (Mullins and Neumann, 1979). In Site 1007 cores, several fragments of ahermatypic corals are imbedded in the drift deposits (Eberli et al., 1997a). Therefore, we infer that the mounds imaged in this study area have a similar composition as those farther north.

The variation in seismic facies described above is clearly related to the distribution of physical properties within the various types of sediments and to their different stages of diagen-

esis (Eberli et al., 1997a); this is also reflected in the checkshot data from four sites along the transect (Fig. 3). Overall acoustic velocity is lowest at Site 1006, which is farthest away from the platform margin. There, a relatively low degree of diagenesis has preserved the original low velocity (Fig. 8). Sites 1003 and 1007 have very similar velocity distributions, so that the overall interval velocity is almost identical (Eberli et al., 1997a). Increased diagenesis in highly indurated layers such as turbidites results in higher velocities at these slope sites than in the drift deposits. Interestingly, the most proximal Site 1005 has higher traveltimes at equal depths and thus lower inter-

val velocities than Sites 1003 and 1007 (Fig. 3). This lower interval velocity is caused by a much thicker and unindurated Pleistocene section at this site (200 m vs. 100 m and 40 m, respectively), which forms an eastward thickening low-velocity wedge (Fig. 4A).

The more distal drift deposits are characterized by a seismic facies with a much higher lateral coherency in contrast to the low seismic coherence in the slope environment. Because of more continuous deposition, reflections in the distal deposits can be easily traced through the entire data set. Contrasted to the sonic log of Site 1003, the log of Site 1006 shows that the variations in sonic velocity—and thus acoustic impedance—are much smaller in the basin than on the slope (Fig. 8). This low and uniform range of acoustic properties is caused mainly by the lack of major diagenetic alterations in the distal areas. Despite the lack of high impedance contrasts, the observed seismic reflectivity is high and regular (Fig. 7C). High lateral continuity compensates for lack of impedance contrast, in particular when an AGC is applied (Anselmetti et al., 1997).

SEISMIC SEQUENCE STRATIGRAPHY

The acquired seismic sections image the carbonate slope and its adjacent basin west of the Neogene platform margin. In distal locations, not all depositional sequences are separated by geometric unconformities, but by their respective conformities. The partly conformable character of sequence boundaries would result in an incomplete number of seismic sequences in this portion of the transect. Therefore, geometric information is needed from farther up the slope, at and beyond the modern platform margin, where the record of geometric unconformities caused presumably by sea-level variations is much more distinct and complete (Sarg, 1988). The cross-bank seismic line (Western Geophysical line) contains this information (Fig. 9) and was used to perform a sequence stratigraphic analysis of the subsurface of Great Bahama Bank by mapping erosional truncations and onlap geometries (Eberli and Ginsburg, 1987, 1989). In addition, the two sites of the Bahamas Drilling Project (Unda and Clino) were both positioned on the Western line, allowing for a calibration of the seismic sequences with lithologic and biostratigraphic data (Eberli et al., 1997b). Seismic line 106, on which ODP Sites 1003–1007 are positioned, retraced the basal portion of the Western line and extended the line farther basinward (Fig. 1). The recognized seismic sequences could be traced from the Western line to line 106 and partition the partly conformable sedimentary succession imaged beneath the Straits of Florida into seismic sequences (Figs. 9 and 10). The seismic correlation between the platform se-

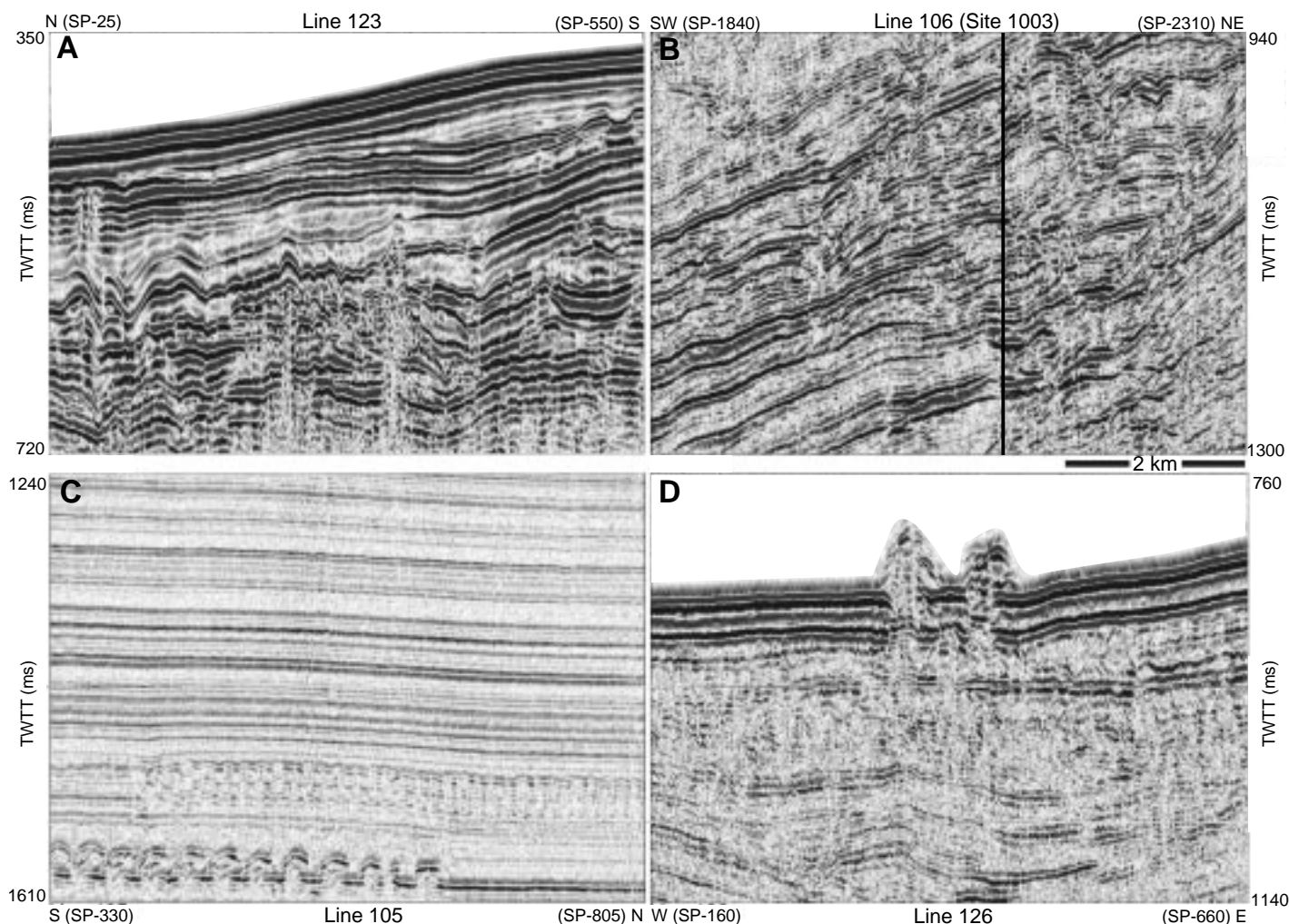


Figure 7. Examples of seismic facies (vertical exaggeration $\sim 15\times$). (A) Margin-parallel seismic section (line 123) with partly chaotic facies of slope sediments. Cut-and-fill geometries are dominant and indicate submarine erosion and deposition processes on the upper slope. (B) Slope facies as in Figure 7A but seen on a dip section (line 106), which emphasizes the partly chaotic and difficult-to-correlate seismic reflection pattern. (C) High-coherent seismic facies of drift deposits as seen on line 105. Although little impedance contrast characterizes the drift deposits, the lateral homogeneity of the layers results in an extremely coherent reflection pattern. Amplitudes, however, are lower, as in the more variable slope deposits. In some cases, the high resolution allows for recognition of prograding sand waves (lower left corner). (D) Examples of mound-shaped lithohermes at the bottom of the Santaren Channel, which likely are formed by deep-water corals.

quences and the slope sequences had to pass underneath the topographically sharp modern platform margin, where numerous diffractions and multiple reflections partly obscure the seismic image. In addition, the Western line was recorded with a lower frequency signal that was used in the high-resolution ODP site survey. Most difficulties occurred for tracing the uppermost Miocene to lowermost Pliocene reflections, where the steep first multiple of the uppermost slope prevented the tracing of the seismic sequence boundaries G, F, and E underneath the modern platform margin. The estimated continuations of these reflections were double checked with the age information from the most proximal drill site 1005 on the upper slope. Despite these difficulties, the sequence

boundaries can be correlated across the entire transect. In fact, the sequence boundaries on the Western line fit well with distinct seismic horizons seen on line 106, so that, together, these two seismic sections provide a complete seismic stratigraphic record of the platform-to-basin transition of Great Bahama Bank from the base of the Neogene to the present.

Seventeen such Neogene seismic sequences are defined across the entire transect (Figs. 9 and 10, and Table 1). They are labeled with italicized, lower-case letters *a* to *q*, and the equivalent basal seismic sequence boundaries are named with non-italicized, capital letters A to Q (for example, M is the seismic sequence boundary at the base of seismic sequence *m*). Seismic sequence *r* is a pre-

Neogene sequence above prominent reflection R.

Comparison of the seismic sequence boundaries with the signature in cores and logs indicates that most sequence boundaries coincide, within seismic resolution of about 10 m, with a facies change indicative of a sea-level change (Eberli et al., 1997a). Figure 11 compares line 106 with the interpreted seismic sequence boundaries and the sonic log at the deepest Site 1007. Log data has the advantage that it is more complete than the seismic data. In particular, the sonic log is a powerful tool to see the presumed effects of relative sea-level variations because the acoustic properties record very sensitively the changes in depositional lithology and diagenetic alterations, both of

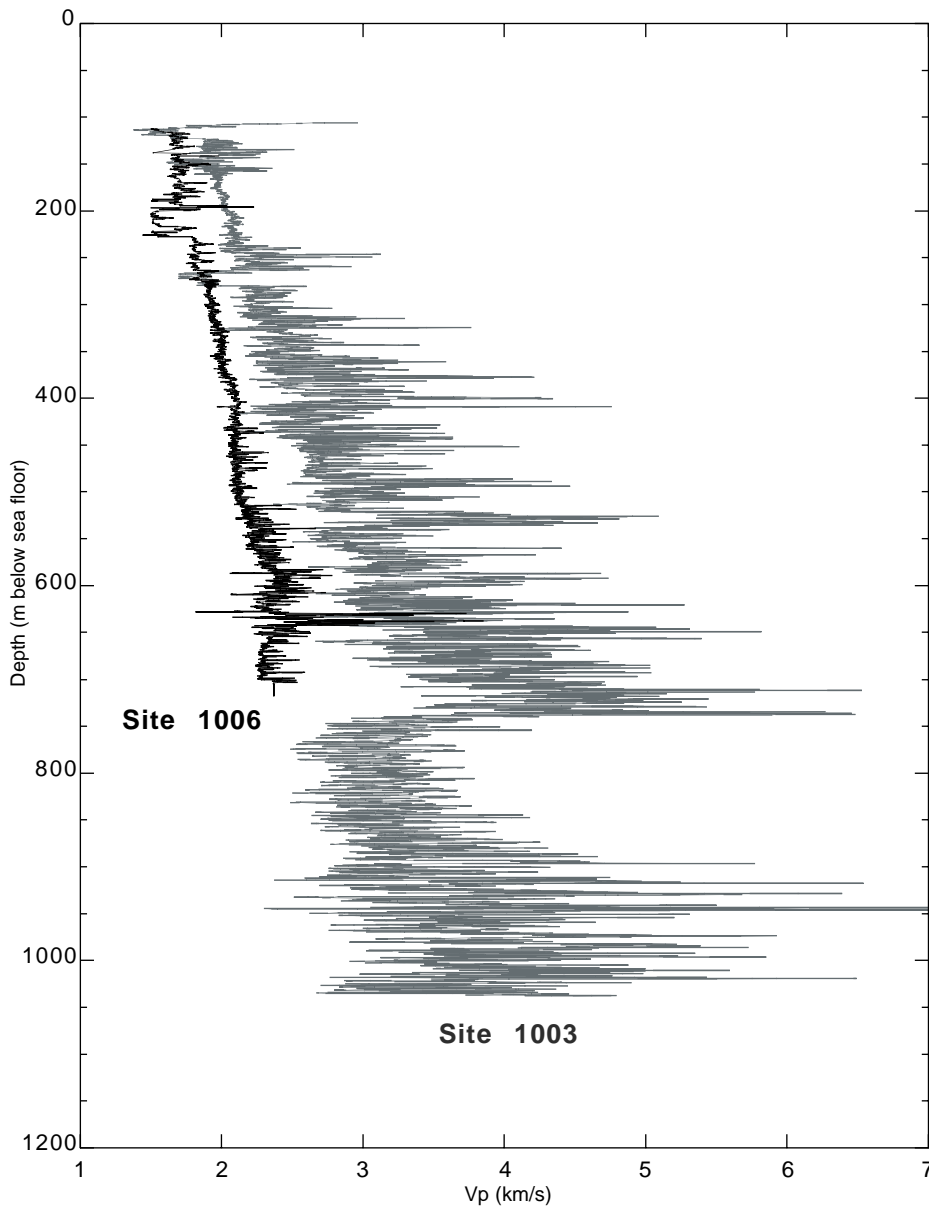


Figure 8. Sonic logs of Ocean Drilling Program Leg 166 Sites 1003 and 1006 (Eberli et al., 1997a). The observed seismic facies (Fig. 7) can be related to the velocity signatures observed in the log. The velocities of the slope deposits at Site 1003 are highly variable, with average velocity contrasts of 2000–3000 m/s, resulting in strong reflectivity contrasts. Only the zone between approximately 150 and 250 m is unconsolidated and results in a characteristic transparent seismic package, as seen in Figures 4 and 5. In contrast to the slope deposits of Site 1003, platform-distal Site 1006 penetrated mostly very homogeneous drift deposits that are characterized by small velocity contrasts of mostly less than 200 m/s. The high lateral coherence of these layers, however, still results in reflectivity contrasts, despite the generally lower reflection amplitudes (see Fig. 7C).

which are strongly influenced by sea-level changes (Anselmetti and Eberli, 1993). Like at the other sites, most of the seismic sequence boundaries at Site 1007 have a distinct signature in the logs, which can be either a sharp peak or a change in log character. Most of the Miocene sequences are characterized by an upward-increasing velocity towards the seismic sequence bound-

ary and a sharp decrease above the boundary (Fig. 11). The Pliocene seismic sequence boundaries, in contrast, show low and uniform velocity values in the upper part of the sequence and a rapid increase of velocity values above the boundary. Despite the fact that few seismic sequence boundaries do not coincide with major petrophysical changes that would indicate lithologic and/or

diagenetic changes (marked on Fig. 11), the good match between seismic sequences and facies changes justifies the use of the seismic sequences as a means to partition the sedimentary record into sea-level-controlled sequences. The 17 seismic sequences detected in the Neogene–Quaternary succession have an average duration of 1–1.5 m.y. (Eberli et al., 1997a). These durations suggest that the seismic sequences along the Bahamas transect record third-order sea-level changes for the Neogene (Vail et al., 1977a).

The following sections describe the seismic signatures of the individual sequences along line 106 together with the seismic characteristics of their unconformities.

Pre-Neogene Sequences

The boundary between Oligocene and Miocene deposits was drilled at ODP Site 1007 at a depth of 1210 mbsf (Eberli et al., 1997a), identified as seismic horizon Q. Most of the pre-Neogene section appears on the seismic profiles below the first sea-floor multiple reflection, so that the primary signal is partly obscured. Several primary high-amplitude, low-frequency reflections, however, can be clearly distinguished within the pre-Neogene strata. These reflections can be seen most prominently on east-west-oriented dip sections, on which they have a different angle than the multiple reflections. On north-south-oriented strike sections, they are parallel to the multiple and thus difficult to discern. Seismic horizon R is the strongest reflection within the pre-Neogene strata and can be traced across the entire seismic grid (Fig. 10). Because neither the sites of the Bahamas Drilling Project on the platform nor the Leg 166 sites in the Straits of Florida penetrated down to this horizon, age assignment of R remains speculative. However, a jump-correlation from the Great Isaac-I well on northern Great Bahama Bank to the Western line and then to line 106 suggests that this reflection is the middle Cretaceous unconformity (Eberli and Ginsburg, 1989). The drilling results of ODP Leg 166 revealed, however, that the sediment package between R and the base of the Neogene (seismic sequence boundary Q) is only approximately 200 m thick. Thus, it seems more likely that R is younger than the middle Cretaceous unconformity. Regardless of its age, the seismic signature of R, which is a high-amplitude and low-frequency couplet of reflections, suggests a significant change in acoustic properties across the horizon.

Miocene Sequences

The Miocene succession is present in 11 seismic sequences, named *q–g* (Fig. 10). Sediments spanning the Oligocene–Miocene boundary were

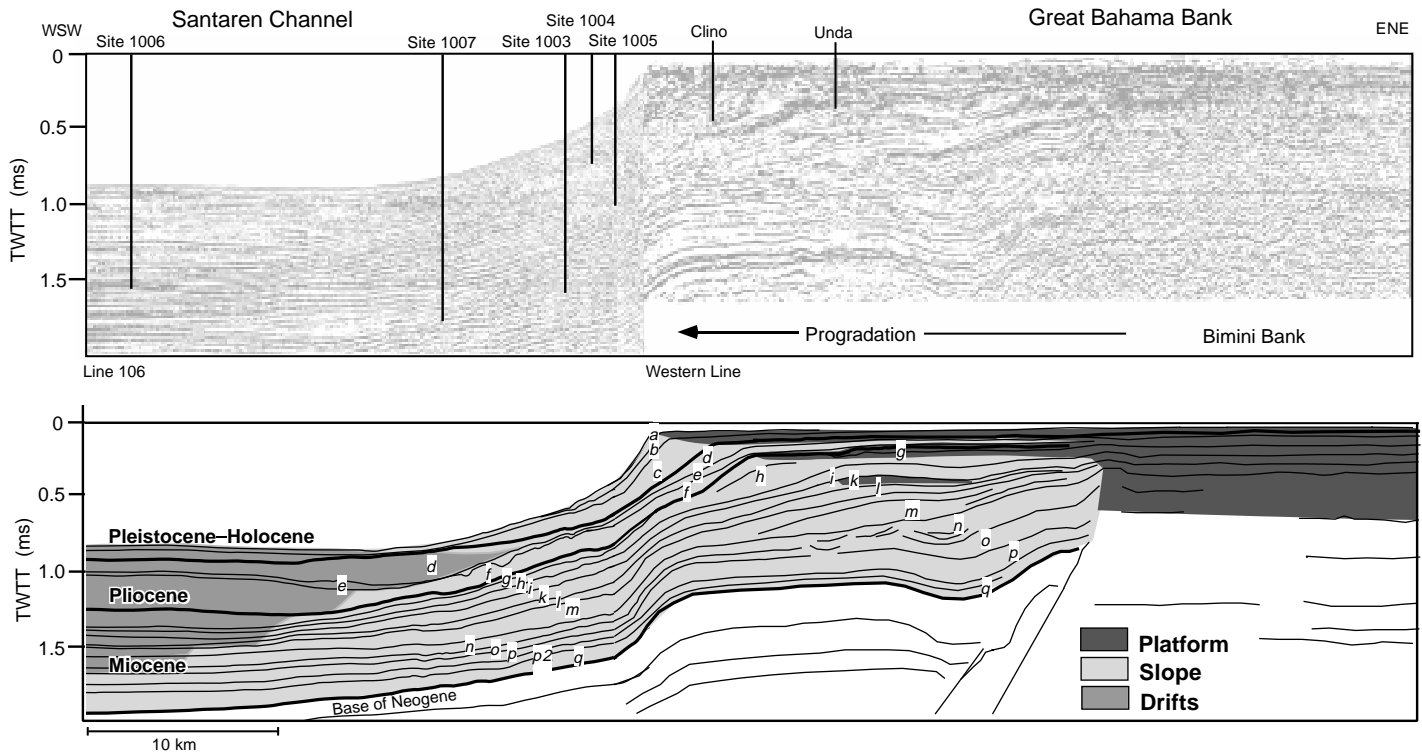


Figure 9. (A) Connection between high-resolution seismic line 106 and the Western Geophysical line on Great Bahama Bank. (B) Interpretation of major depositional and seismic facies for line 106 and Western line. Both lines lie along the same trend (Fig. 1). Seismic sequence boundaries were defined in the subsurface of the platform in the east and then extended into the basin (modified after Eberli et al., 1997a).

drilled and dated biostratigraphically at Site 1007 so that this boundary was identified seismically and traced across the entire transect. On the seismic data at Site 1007, a prominent reflection appears at 1190 mbsf (Table 1), which is 20 m above the biostratigraphic marker that indicates the base of the Miocene. Shipboard measurements indicate that this reflection is caused by a sharp increase in velocity at 1190 mbsf (Fig. 11). Thus, the seismic sequence boundary Q marks a horizon 20 m above the biostratigraphic base of the Miocene. Nevertheless, we name Q the seismic base of the Miocene, recognizing, however, that the Oligocene-Miocene boundary is just below this reflection.

The early and the late Miocene each consist of three seismic sequences ($q-p$ and $l-g$, respectively), whereas five sequences ($o-k$) can be identified in the middle Miocene. The age of seismic sequence boundary O correlates with the early-late Miocene boundary, and seismic sequence boundary I marks the middle-late Miocene boundary. Most seismic sequences of the early and middle Miocene show a gradual lateral transition from a slope part, characterized by irregular reflection geometries, to more seismically continuous deposits in the platform-distal areas. The slope sections are generally thicker than the basinal sections, indicating that deposition during

this time is concentrated on the slope. All the Miocene sequences are characterized by rather subtle downlapping reflections oriented towards the west, which are caused by prograding base-of-slope sediments. These downlap surfaces generally coincide with the seismic sequence boundary, but, due to the high resolution, additional downlap surfaces can be detected within the sequences. The slope part of the sequences shows abundant small-scale erosional surfaces due to the active downslope sediment transport.

Middle Miocene sequence k and late Miocene sequences $i-g$ are the first sequences in which the basinal sections become thicker than the slope sections (Fig. 10). This reversal is caused by the growing dominance of drift deposits. The youngest Miocene seismic sequence (g) shows, in addition to the thickening, several distinct downlapping reflections towards the northeast that result from progradation of the drift deposits. Unlike the older Miocene sequences, in which sedimentation is nearly equal between slope and basin, sequence g forms the base of a sediment wedge the reflections of which terminate onto lower-slope sediments, indicating incomplete or reduced sedimentation on the slope. Sequence g , in fact, thins significantly eastward towards the modern platform margin. This observed seismic thinning correlates well with the

fact that, even farther to the east, drill hole Clino penetrated a horizon that represents a long hiatus spanning the Miocene-Pliocene boundary, indicating that the time-equivalent strata composing sequence g are missing higher up on the slope (Eberli et al., 1997b).

Pliocene Sequences

Unlike the Miocene section, the Pliocene section, which consists of three seismic sequences ($f-d$), shows a more distinct seismic separation between slope and basinal sediments (Fig. 10). The transition between the two depositional systems is characterized by unconformities associated with reflection terminations and not simply by a gradual transition. For example, the slope part of sequence f is an incised and seismically transparent unit. In contrast, this interval is characterized in the basin by a thick and very coherent succession of drift deposits (Figs. 4 and 10). The reflections of these drift deposits wedge out at the base-of-slope with downlaps towards the transparent slope unit. Biostratigraphic dating at Site 1007 showed that the top of f is marked by a hiatus spanning the early-late Pliocene boundary, indicating erosion or bypass sedimentation at that time (Eberli et al., 1997a). Farther up the slope at Sites 1003–1005, sequence f becomes

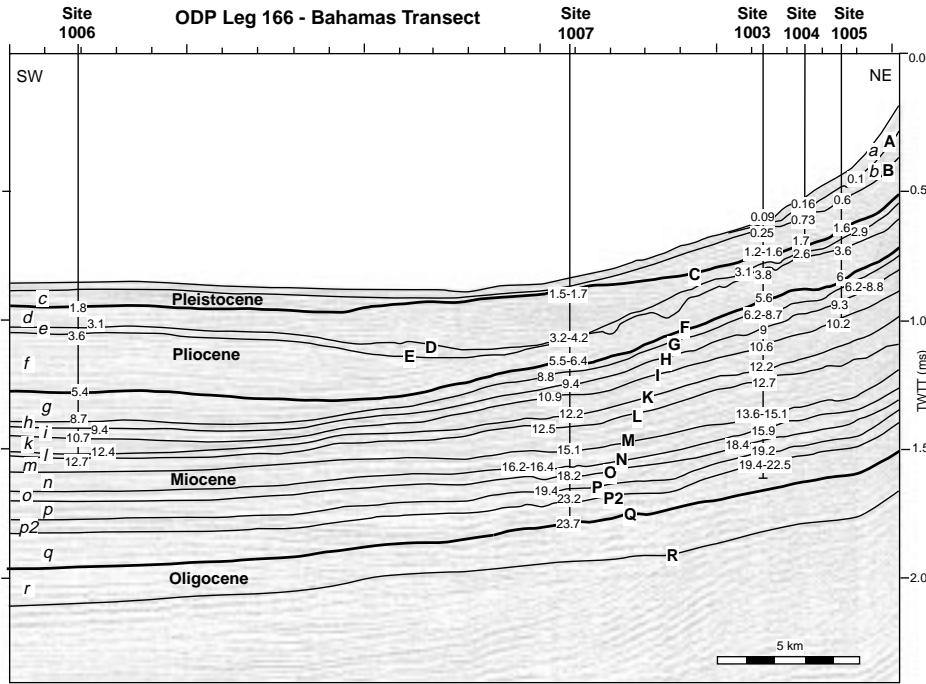


Figure 10. Seismic sequence boundaries correlated between the western line into line 106 (vertical exaggeration ~10x). The 17 seismic sequences could be traced across the entire transect. Site 1007 penetrated the entire Neogene–Quaternary succession by reaching the base of the Neogene, marked with seismic sequence boundary Q (modified after Eberli et al., 1997a). The numbers indicate the ages (m.y.) of the seismic sequence boundaries at each drill site obtained by combining the best-fit biostratigraphic age-depth curves with the two-way-traveltime depth curves from the checkshot surveys.

thicker and more complete in stratigraphic terms, documenting more continuous sedimentation on the middle and upper slope (Fig. 10). Because of its transparent seismic facies and incised nature (Figs. 4, 5, and 10), no precise geometric unconformities and correlations can be recognized within the slope part. At the toe-of-slope, erosion of the top of sequence *f* creates a north-south-oriented channel (Fig. 6), which was likely partly created by bottom-current erosion parallel to the slope. This erosion can be recognized by the truncation of reflections of the youngest drift deposits, yielding an erosional unconformity at seismic sequence boundary E that results in a channel-like morphology (Fig. 6). This erosion caused part of the observed hiatus at Site 1007. The overlying sequence *e* infills this depression and inverts the relief with deposits that form a mound-like geometry with downlap in both platformward and basinward directions (Fig. 10). In addition to infilling the slope-parallel channel, sequence *e* also infills all incised canyons that were eroded on the slope into underlying sequence *f*. Being mainly restricted to these former depressions, sequence *e* thins out towards Site 1007, increasing the observed hiatus spanning the early-late Pliocene boundary at Site 1007. The good match between seismic sequence boundaries and biostratigraphic data is indicated by the merging of seismic sequence boundaries E and D at Site 1007 (Fig. 11).

During deposition of the youngest Pliocene sequence (*d*), the depocenter moved eastward towards the base-of-slope, approximately to the position of Site 1007. The sediments of *d* gently

TABLE 1. DEPTHS AND AGES OF SEISMIC SEQUENCE BOUNDARIES

SSB	Age of boundary	Composite age* (Ma)	Maximum age offset† (Ma)	Site 1006		Site 1007		Site 1003		Site 1004		Site 1005	
				TWTT (ms)	Depth (mbsf)	TWTT (ms)	Depth (mbsf)	TWTT (ms)	Depth (mbsf)	TWTT (ms)	Depth (mbsf)	TWTT (ms)	Depth (mbsf)
A	Pleistocene–Holocene (?)	0.1	0.07	N.D.	N.D.	N.D.	N.D.	10	8	20	15	25	20
B		0.6	0.5	N.D.	N.D.	N.D.	N.D.	30	25	70	65	100	90
C		1.7	0.2	100	90	40	35	110	100	160	150	200	185
D	Pliocene–Pleistocene	3.1	0.6	160	145	220	210	150	145	200	185	240	225
E		3.6	0.2	190	170	220	210	180	175	220	205	270	255
F	Miocene–Pliocene	5.4	0.6	410	380	310	310	315	315			400	400
G		8.7	0.1	530	505	350	365	340	350			430	430
H	Middle–late Miocene	9.4	0.4	550	530	390	420	380	400			475	485
I		10.7	0.7	585	570	440	490	475	520			520	550
K		12.2	0.2	660	660	520	600	570	670				
L		12.7	0.2	675	675	570	670	610	740				
M	Early–middle Miocene	15.1	0.0			660	810	725	915				
N		15.9	0.3			720	900	790	1025				
O		18.3	0.2			760	960	840	1105				
P		19.4	0.2			800	1020	880	1165				
P2		23.2	0.7			860	1115	900	1190				
Q	Oligocene–Miocene	23.7	N.A.			910	1190						
R	?					1080	1460 [§]						

Notes: SSB—seismic sequence boundary. Depth of SSB is given in milliseconds (ms) of two-way traveltime (TWTT) and in meters below seafloor (mbsf). Depth in meters was obtained through time-to-depth conversion (Fig. 3) from checkshot survey at four sites. N.D.—seismically not detectable. N.A.—not available (could not be determined).

*The composite age is the averaged biostratigraphic age of the SSB across the entire transect (see Eberli et al., 1997a).

†See Figure 10. The maximum age offset is the maximum difference in age of one SSB between all sites where the SSB was drilled and dated.

§Estimated (not drilled).

#Average Δt.

thin out towards the west, as well as towards the slope. Reflections within seismic sequence *d* merge together upslope of Site 1007 and show terminations at the base of the sequence, forming an onlap surface between Sites 1007 and 1003 along seismic sequence boundary D (Fig. 10). Biostratigraphic data, however, suggest that this onlap is rather an effect of the layers thinning below the limits of seismic resolution, because sedimentation at Sites 1003–1005 on the late Pliocene slope is strongly condensed but nearly continuous (Eberli et al., 1997a). The observed onlap surface at the base of *d* would thus be a pseudo-unconformity, as shown in other examples of seismically modeled carbonate slopes (Stafleu and Sonnenfeld, 1994; Stafleu et al., 1994; Anselmetti et al., 1997).

Pleistocene–Holocene Sequences

The Quaternary succession consists of three seismic sequences (*c–a*); all contain thick units at the platform margin (Fig. 9). This is a result of a regression of the base-of-slope that produces steepening of the slope angle. Sequences *a* and *b* cannot be resolved in the distal parts of the Straits of Florida, because their vertical extent is below that of seismic resolution; in addition, they are partly masked by some shallow ghosts of the seismic signal in the uppermost few meters of the seafloor sediments. A slight increase in thickness of sequence *c* at the basin floor, however, indicates that drift sediments were still being deposited by the Florida Current during the Quaternary.

In addition to a geometry that is characterized by erosive downslope channels, all three sequences show distinct downlapping surfaces that resulted from the basinward termination of steep beds of slope sediments. They form a sharp edge today, as shown in previous seismic investigations (Wilber et al., 1990). For seismic sequence boundary C, these slope sediments terminate approximately at the position of Site 1007. The front of these downlapping slope wedges back-steps throughout the Quaternary to its present position, between Sites 1003 and 1004 (Fig. 10). The uppermost sequence *a*, is likely a product of the last sea-level highstand of the Holocene, though no precise biostratigraphic dating was possible for seismic sequence boundary A (Eberli et al., 1997a).

Chronostratigraphic Significance of Seismic Reflections

One of the basic assumptions of seismic sequence stratigraphy is that seismic reflections—and in particular seismic sequence boundaries—do not crosscut time lines and therefore have chronostratigraphic significance (Vail et al.,

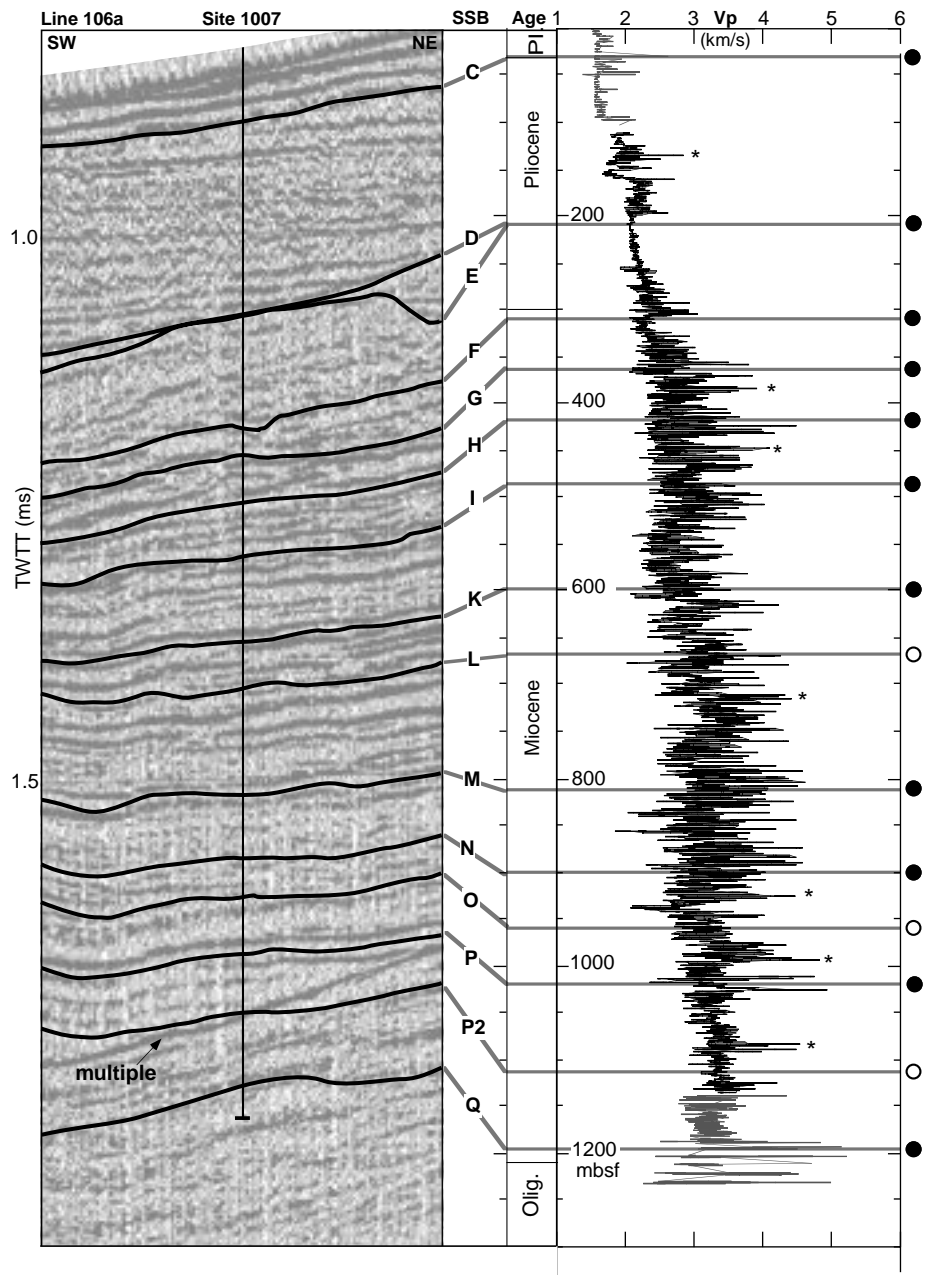


Figure 11. Match between seismic section, seismic sequence boundaries (SSB), and petrophysically and lithologically significant markers recognized in the sonic log of Site 1007 (modified after Eberli et al., 1997a). Most SSBs coincide in the log with distinct changes in acoustic signature (marked by solid circles at right side). In the Miocene section, the SSBs generally display a gradual upward increase of velocity within the sequence and an abrupt upward decrease across the boundary. Pliocene SSBs F–D are characterized acoustically by low, constant velocity values below and by a rapid velocity increase above the boundary. Some SSBs do not necessarily coincide with major changes in physical or lithologic properties (marked by open circles). In addition, some major peaks in the sonic log signature do not match, within seismic resolution, with a SSB. This might indicate higher-order cyclicity in the sedimentation pattern (marked by *). The top and bottom 100 m of the sonic log (gray curve) were reconstructed using Ocean Drilling Program shipboard core-velocity measurements, because no sonic log was available.

1977b). Several studies of seismic modeling, however, have shown that under certain circumstances, this precondition might sometimes be violated (Tipper, 1993; Staffeu and Sonnenfeld, 1994; Staffeu et al., 1994). However, not many extensive data sets exist that can date high-resolution seismic reflection events using data from continuously cored drill holes. The high-resolution seismic line 106, together with the five continuously cored drill holes and the precise time-to-depth conversions from four checkshot surveys (Fig. 3), now provide a unique opportunity to date seismic reflections and to correlate their biostratigraphic ages across the entire transect. Therefore, comparison of the seismic interpretation with biostratigraphic core data represents a test of the seismic sequence-stratigraphic concept for the investigated carbonate-platform-margin setting. The ages of the drilled cores of ODP Leg 166 were determined by the Scientific Shipboard Party (Eberli et al., 1997a) using calcareous nannofossils and planktonic foraminifers. By establishing a two-way travelttime-to-depth conversion from the accurate checkshot surveys (Fig. 3), it became possible to assign ages to each seismic sequence boundary at all sites where they were drilled. Figure 10 displays these ages and shows the variation in age across the transect. In fact, the average difference in resulting ages of all seismic sequence boundaries at each site (Table 1) amounts to 0.32 m.y. (Eberli et al., 1997a) and thus lies within the combined range of seismic and biostratigraphic resolution. It is remarkable that all Neogene seismic horizons are also chronostratigraphic boundaries from the middle of the Santaren Channel up to the Great Bahama Bank, reaffirming the hypothesis that seismic reflections and their associated seismic sequence boundaries represent time lines. Consequently, even the drift deposit maintains its biostratigraphic integrity, despite the fact that the sediment was reworked by contour-following ocean currents after the material was transported downslope. The seismic sequence boundaries correlate across the depositional facies transitions without changing their chronostratigraphic identity.

EVOLUTION OF THE PLATFORM-TO-BASIN TRANSITION THROUGH TIME

The densely spaced grid of two-dimensional seismic sections allows for a general three-dimensional analysis of the platform margin architecture (Fig. 2). All major time boundaries could be located on the seismic sections using biostratigraphic and checkshot data from ODP Leg 166 sites. Because the seismic sequence boundaries are in fact chronostratigraphically significant horizons, it was possible to correlate the age markers across the entire seismic grid. Interpolations

between seismic sections, done by the seismic interpretation software, resulted in a detailed three-dimensional image of the sediment bodies of all major epochs. The isopach maps of the lower, middle, and upper Miocene, the lower and upper Pliocene, and the Pleistocene–Holocene packages are shown in Figure 12. They document the depositional evolution of this platform-to-basin transition through time.

Figure 12 (A–C) shows the thicknesses of the sediments for each of the three Miocene ages. The thickness is given in milliseconds of two-way-traveltime, which is converted to approximate thicknesses in meters by using the displayed correlation, assuming an average velocity of 2600 m/s. The isopachs are all oriented north-south, parallel to the platform margin. Widely spaced isopachs document a rather uniform thickness of lower Miocene sediments (Fig. 12A). During this time, the platform margin was farther east of the current margin, so that no direct topographic effect of the platform slope is recorded. In contrast to this more uniform sediment distribution, the isopach map of the middle Miocene (Fig. 12B) shows an increase towards the east as a result of the westward progradation of the platform margin (Eberli and Ginsburg, 1989). This simple eastward thickening and wedge-like sediment distribution became more complicated in the late Miocene (Fig. 12C). In the paleo-Straits of Florida, a second depocenter became active, suggesting the onset of drift deposition after 12.4 Ma. The slope and the Straits depocenters are separated by an area of reduced deposition, located at the toe-of-slope (Fig. 6).

The deposition of drift deposits in the Straits of Florida became more pronounced during the early Pliocene (Fig. 12D), when the bulk of the sediment was shed into the basin and redistributed by ocean currents. The thick package of lower Pliocene drift deposits thins out quickly towards the east, while sedimentation on the slope became irregular, presumably due to the intense erosion processes creating the submarine canyons on the slope (Figs. 5, 6, and 12D). During the late Pliocene, the depocenter of the drift deposits shifted approximately 10 km eastward (Fig. 12E), completely infilling the depression created between the upper Miocene–lower Pliocene drifts and time-equivalent slope deposits. Infilling of this depression at the toe-of-slope (Fig. 6) resulted in an inversion of topography, so that, by the end of the Pliocene, the former channel formed a ridge-like topography (Fig. 10). Slope sedimentation was strongly condensed during the entire late Pliocene, when most of the sediments that were shed from the platform top bypassed the slope and accumulated farther out in the basin.

The Pleistocene and Holocene sections show a very narrow but thick wedge of slope deposits close

to the platform margin (Fig. 12F). Drift deposition, which was dominant in the Pliocene, was reduced. A slight westward thickening of sediments in the distal areas was still occurring, however, indicating ongoing deposition by recent currents.

The overall slope angle increases through time over the entire Miocene to Holocene section, from a gentle slope at the base of the Neogene (2° – 4°) to the steep modern value formed by the Pleistocene–Holocene wedge of upper slope sediments (6° – 9°). In addition, the uppermost portion of the modern margin is a near-vertical cliff of ~60 m relief (Wilber et al., 1990). Because of this steepening, the toe-of-slope moved progressively farther to the east while the platform margin continued to prograde westward. Consequently, the whole slope area became narrower and, despite the oversteepening of the margin, yielded a widening of the basin floor during much of the Neogene.

SUMMARY AND CONCLUSIONS

The results of the seismic survey of the platform-to-basin transition of Great Bahama Bank show that two major depositional processes controlled the sediment distribution west of the modern platform margin. Downslope currents transported the sediment that was produced on the platform top onto the slope and into the basin, partly through a series of submarine canyons. Sediments that were not deposited on the slope but shed into the basin were redistributed by ocean currents—for example, by the Florida Current—yielding thick packages of drifts in the distal areas.

Both of these processes were directly linked to sea-level variations, because shallow-water carbonates are generally not produced during sea-level lowstands. In fact, drilling results of ODP Leg 166 indicate that, while lowstand deposition on the slope is strongly reduced or halted, basinal sections still received some drift deposits that are characterized by a more clay-rich, low-carbonate composition (Eberli et al., 1997a). Consequently, the interfingering of the two systems provides an edifice that records the sea-level signal across the entire platform margin. The record of sea-level changes in the drift deposits is mostly given by sediment composition and thickness. Sedimentary load carried by the Florida Current was derived largely from the adjacent platforms; this load was greatly reduced during sea-level lowstands. Furthermore, lowering of sea level likely restricted the current to a narrower strait, causing a faster flow and possibly enhanced sea-floor erosion (Richardson et al., 1969). We postulate that both the observed unconformities on the slope and also those seen in the basinal drift packages were sea-level controlled.

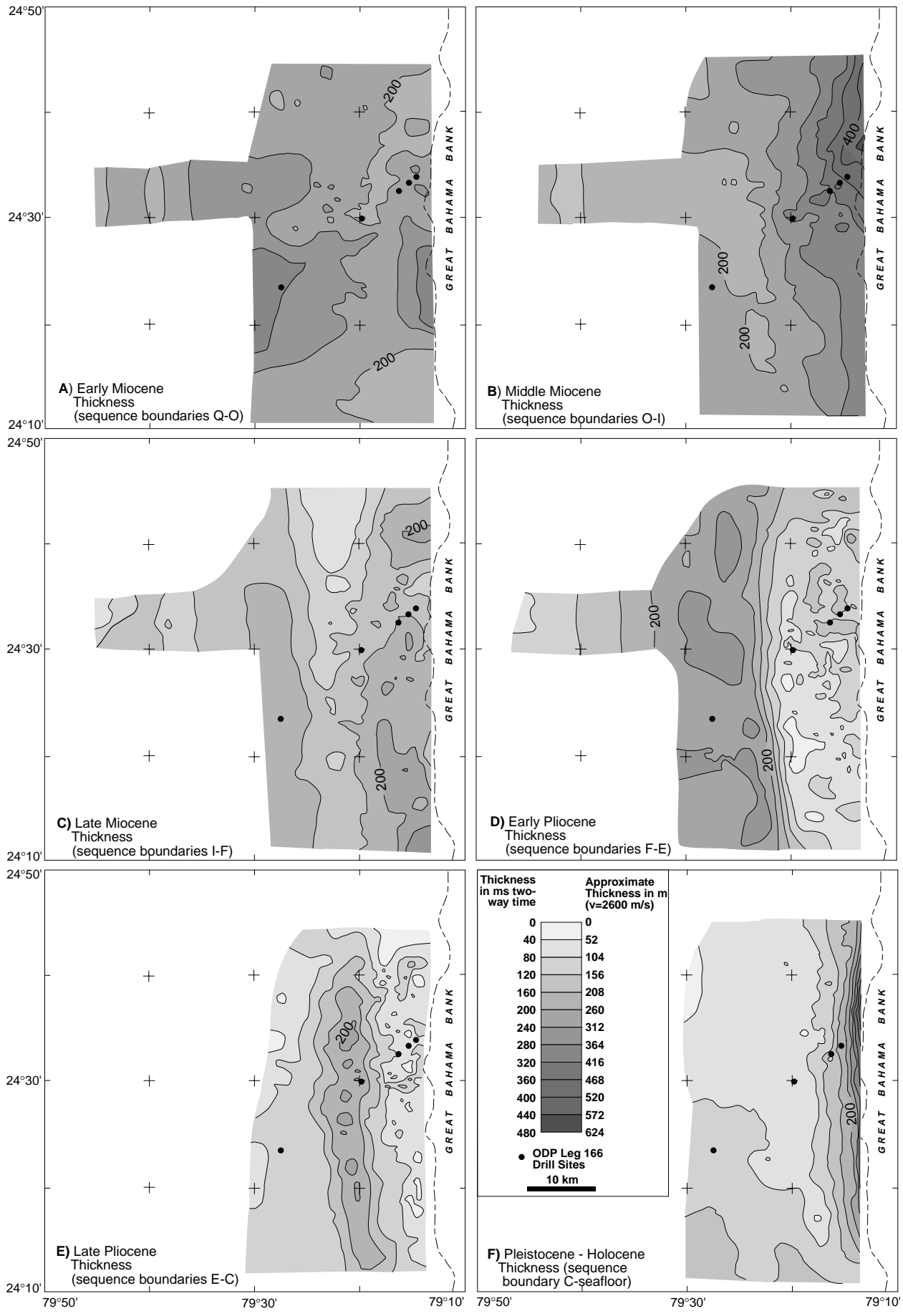


Figure 12. Isopach maps (in milliseconds of two-way traveltime) of six depositional periods documenting the shift of depocenters through time. Shaded patterns denote by intervals two-way traveltime (m/s) and approximate thickness (m) for (A) early Miocene, (B) middle Miocene, (C) late Miocene, (D) early Pliocene, (E) late Pliocene, and (F) Pleistocene–Holocene. Sedimentation rates during the Miocene (A–C) were more uniform overall than during the younger stages (D–F). The middle Miocene (B), however, displays higher sedimentation rates on the slope closer to the platform. The early Pliocene map (D) indicates a sharp increase in sedimentation in the western zones, where a thick wedge of drift sediments is deposited. The eastern limit of the wedge ends rather abruptly, resulting in close-spaced isopachs. During the late Pliocene (E), the depocenter of the drift deposits shifts eastward and infills the topographic depression created by the early Pliocene drifts. In the Pleistocene (F), the depocenter moves further eastward to the upper slope of the platform. The platform margin continuously steepens and more sediment is kept at a margin-proximal position, while less sediment is transported basinward.



The chronostratigraphic integrity of the interfingering geometry is confirmed by the synchronism of seismic reflections and associated seismic sequence boundaries across the entire transect, as determined by biostratigraphic dating at all ODP Leg 166 sites. The ages of the same reflections vary from basin to platform within seismic or biostratigraphic resolution, thus confirming one of the major assumptions of seismic sequence stratigraphy. The seismic sequence analysis, yielding 17 Neogene to Quaternary sequences, provides the means to partition the whole platform margin-to-basin system into sea-level controlled sequences.

The average duration of 1–1.5 m.y. for the sequences suggests that the chosen high-resolution seismic surveying method has the potential to detect third-order sea-level changes from the base of the Neogene to the Quaternary. In addition to reconstructing the sea-level history, the drift deposits also provide information about the history and evolution of Florida Current. The seismically recognized onset of drift deposition in the middle Miocene, which persists to the present, might record the onset of the modern conveyor-type circulation in the Atlantic.

ACKNOWLEDGMENTS

The seismic data acquisition and interpretation were funded by National Science Foundation (NSF) grant OCE-9314586 (to Eberli, D.F. McNeill, and P.K. Swart). This grant included a sub-contract to Rice University for data acquisition on the R/V *Lone Star*. Andre Droxler and John Anderson tailored the acquisition system to fit our needs. We thank John Anderson and the crew of the *Lone Star*, especially Captain Mark Herring, for their dedication. Without the technical skills of Dave Mucciarone (Rice University) and Christian Palud (CEROCEAN, France), the data acquisition would not have been completed successfully. Andre Droxler gave valuable input to the planning of the cruise, in assembling the necessary equipment, and in acquiring data during the initial phase of the investigation. He also brokered the use of the GI airgun and the Triton-Elics system, which were given to us for free for the duration of the cruise by Robert Girault. Don McNeill and Dominic Esker helped during the data acquisition and endured some severe weather. The first 16 months of Anselmetti's stay at the University of Miami were funded by a grant from the Swiss National Science Foundation.

Interpretation of the data was performed with the Landmark software package that was provided to the University of Miami by the vendor. An upgrade of the seismic processing facility at the Rosenstiel School of Marine and Atmospheric Science by NSF grant OCE-9615141 (to C. Scholz and Eberli) improved the data presentation.

Ground truth measurements of the seismic data was provided by the cores recovered during ODP Leg 166. We thank the Scientific Shipboard Party and the technical staff on the *JOIDES Resolution* for all their input.

The manuscript benefited significantly by comments and suggestions from Associate Editor Don McNeill and reviewers Jamie Austin and Chuck Holmes.

REFERENCES CITED

- Anselmetti, F.S., and Eberli, G.P., 1993, Controls on sonic velocity in carbonates: *Pure and Applied Geophysics*, v. 14, p. 287–323.
- Anselmetti, F.S., Eberli, G.P., and Bernoulli, D., 1997, Seismic modeling of a carbonate platform margin (Montagna della Maiella, Italy): Variations in seismic facies and implications for sequence stratigraphy, in Palaz, I., and Marfurt, K.J., eds., *Carbonate seismology: Society of Economic Geologists Geophysical Developments Series*, v. 6, p. 373–406.
- Austin, J.A., Jr., Ewing, J.I., Ladd, J.W., Mullins, H.T., and Sheridan, R.E., 1988, Seismic stratigraphic implications of ODP Leg 101 site surveys, in Austin, J.A., Jr., and Schlager, W., eds., *Proceedings of the Ocean Drilling Program, scientific results, Leg 101: College Station, Texas, Ocean Drilling Program*, v. 101, p. 391–424.
- Berggren, W.A., Kent, D.V., Swisher, C. C., III, and Aubry, M.-P., 1995, A revised Cenozoic geochronology and chronostratigraphy, in Berggren, W.A., Kent, D.V., and Hardenbol, J., eds., *Geochronology, time scales and*

global stratigraphic correlations: A unified temporal framework for an historical geology: *SEPM (Society for Sedimentary Geology) Special Volume 54*, p. 129–212.

- Brunner, C.A., 1984a, Deposition of a muddy sediment drift in the southern Straits of Florida during the Quaternary: *Marine Geology*, v. 69, p. 235–249.
- Brunner, C.A., 1984b, Evidence for increased volume transport of the Florida Current in the Pliocene and Pleistocene: *Marine Geology*, v. 54, p. 223–235.
- Crevello, P.D., and Schlager, W., 1980, Carbonate debris sheets and turbidites, Exuma Sound, Bahamas: *Journal of Sedimentary Petrology*, v. 50, p. 1121–1148.
- Denny, W., Austin, J.A., and Buffler, R.T., 1994, Seismic stratigraphy and geologic history of mid-Cretaceous through Cenozoic rocks, southern Straits of Florida: *American Association of Petroleum Geologists Bulletin*, v. 78, p. 461–487.
- Eberli, G.P., 1988, Physical properties of carbonate turbidite sequences surrounding the Bahamas: Implications for slope stability and fluid movements, in Austin, J.A., Jr., and Schlager, W., eds., *Proceedings of the Ocean Drilling Program, scientific results, Leg 101: College Station, Texas, Ocean Drilling Program*, v. 101, p. 305–314.
- Eberli, G.P., and Ginsburg, R.N., 1987, Segmentation and coalescence of Cenozoic carbonate platforms, northwestern Great Bahama Bank: *Geology*, v. 15, p. 75–79.
- Eberli, G.P., and Ginsburg, R.N., 1989, Cenozoic progradation of northwestern Great Bahama Bank, a record of lateral platform growth and sea-level fluctuations, in Crevello, J.L., Wilson, J.L., Sarg, J.F., and Read, J.F., eds., *Controls on carbonate platform and basin development: Society of Economic Paleontologists and Mineralogists Special Publication 44*, p. 339–351.
- Eberli, G.P., Swart, P.K.S., and Malone, M., et al., 1997a, Proceedings of the Ocean Drilling Program, initial reports, Leg 166: College Station, Texas, Ocean Drilling Program, v. 166, 850 p.
- Eberli, G.P., Swart, P.K., McNeill, D.F., Kenter, J.A.M., Anselmetti, F.S., Melim, L.A., and Ginsburg, R.N., 1997b, A synopsis of the Bahamas Drilling Project: Results from two deep core borings drilled on the Great Bahama Bank, in Eberli, G.P., Swart, P.K., and Malone, M., et al., *Proceedings of the Ocean Drilling Program, initial reports, Leg 166: College Station, Texas, Ocean Drilling Program*, v. 166, p. 23–41.
- Glaser, K.S., and Droxler, A.W., 1991, High production and highstand shedding from deeply submerged carbonate banks, northern Nicaragua Rise: *Journal of Sedimentary Petrology*, v. 61, p. 128–142.
- Harwood, G.M., and Towers, P.A., 1988, Seismic sedimentologic interpretation of a carbonate slope, north margin of Little Bahama Bank, in Austin, J.A., Jr., Schlager, W., et al., *Proceedings of the Ocean Drilling Program, scientific results, Leg 101: College Station, Texas, Ocean Drilling Program*, v. 101, p. 263–277.
- Hine, A.C., Wilber, R.J., Bane, J.M., Neumann, A.C., and Lorenson, K.R., 1981, Offbank transport of carbonate sands along open, leeward bank margins: Northern Bahamas: *Marine Geology*, v. 42, p. 327–348.
- Jordan, G.F., Malloy, R.J., and Kofoed, J.W., 1964, Bathymetry and geology of Pourtales Terrace, Florida: *Marine Geology*, v. 1, p. 259–287.
- Kaneps, A.G., 1979, Gulf Stream: Velocity fluctuations during the late Cenozoic: *Science*, v. 204, p. 297–301.
- Ladd, J.W., and Sheridan, R.E., 1987, Seismic stratigraphy of the Bahamas: *American Association of Petroleum Geologists Bulletin*, v. 71, p. 719–736.
- McCave, I.N., and Tucholke, B.E., 1986, Deep current-controlled sedimentation in the western North Atlantic, in Vogt, P.R., and Tucholke, B.E., eds., *The western North Atlantic region: Geological Society of America, Geology of North America*, v. M, p. 451–468.
- Mountain, G.S., and Tucholke, B.E., 1989, Abyssal sediment waves, in Bally, A.W., ed., *Atlas of seismic stratigraphy: American Association of Petroleum Geologists Studies in Geology*, v. 27, no. 3, p. 233–236.
- Mullins, H.T., 1983, Modern carbonate slope and basins of the Bahamas, in Cook, H.E., Hine, A.C., and Mullins, H.T., eds., *Platform margin and deepwater carbonates: Society of Economic Paleontologists and Mineralogists Course 12*, p. 4.1–4.138.

- Mullins, H.T., and Neumann, A.C., 1979, Deep carbonate bank margin structure and sedimentation in the northern Bahamas, in Doyle, L.J., and Pilkey, O.H., eds., *Geology of continental slopes: Society of Economic Paleontologists and Mineralogists Special Publication 27*, p. 165–192.
- Mullins, H.T., Neumann, A.C., Wilber, R.J., Hine, A., and Chinburg, S.J., 1980, Carbonate sediment drifts in the northern Straits of Florida: *American Association of Petroleum Geologists Bulletin*, v. 64, p. 1701–1717.
- Mullins, H.T., Heath, K.C., Van Buren, H.M., and Newton, C.R., 1984, Anatomy of modern open-ocean carbonate slope: Northern Little Bahama Bank: *Sedimentology*, v. 31, p. 141–168.
- Mullins, H.T., Gardulski, A.F., Wise, S.W., Jr., and Applegate, J., 1987, Middle Miocene oceanographic event in the eastern Gulf of Mexico: Implications for seismic stratigraphic succession and Loop Current/Gulf Stream circulation: *Geological Society of America Bulletin*, v. 98, p. 702–713.
- Pinet, P.R., and Popenoe, P., 1985, A scenario of Mesozoic–Cenozoic ocean circulation over the Blake Plateau and its environments: *Geological Society of America Bulletin*, v. 96, p. 618–626.
- Raymo, M.E., Hodell, D., and Jansen, E., 1992, Response of deep ocean circulation to initiation of Northern Hemisphere glaciation (3–2 Ma): *Paleoceanography*, v. 78, p. 645–672.
- Richardson, W.S., Schmitz, W.J., Jr., and Nüiler, P.P., 1969, The velocity structure of the Florida Current from the Straits of Florida to Cape Fear: *Deep-Sea Research*, v. 16, p. 225–231.
- Sarg, J.F., 1988, Carbonate sequence stratigraphy, in Wilgus, C.K., Hastings, B.S., Kendall, C.G.St.C., Posamentier, H.W., Ross, C.A., and Van Wagoner, J.C., eds., *Sea-level changes: An integrated approach: Society of Economic Paleontologists and Mineralogists Special Publication 42*, p. 155–188.
- Schlager, W., 1981, The paradox of drowned reefs and carbonate platforms: *Geological Society of America Bulletin*, v. 92, p. 197–211.
- Schlager, W., and Chermak, A., 1979, Sediment facies and of platform basin-transition, Tongue of the Ocean, Bahamas, in Doyle, L.J., and Pilkey, O.H., *Geology of continental slopes: Society of Economic Paleontologists and Mineralogists Special Publication 27*, p. 193–207.
- Schlager, W., Hooke, R.L., and James, N.P., 1976, Episodic erosion and deposition in the Tongue of the Ocean, Bahamas: *Geological Society of America Bulletin*, v. 87, p. 1115–1118.
- Schlager, W., Bourgeois, F., MacKenzie, G., and Smit, J., 1988, Boreholes at Great Isaac and Site 626 and the history of the Florida Straits, in Austin, J.A., Jr., Schlager, W., et al., *Proceedings of the Ocean Drilling Program, scientific results, Leg 101: College Station, Texas, Ocean Drilling Program*, v. 101, p. 425–437.
- Sheridan, R.E., Crosby, J.T., Bryan, G.M., and Stoffa, P.L., 1981, Stratigraphy and structure of southern Blake Plateau, northern Florida Straits, and northern Bahama Platform from multichannel seismic reflection data: *American Association of Petroleum Geologists Bulletin*, v. 65, p. 2571–2593.
- Stafleu, J., and Sonnenfeld, M.D., 1994, Seismic models of a shelf-margin depositional sequence: Upper San Andres Formation, Last Chance Canyon, New Mexico: *Journal of Sedimentary Research*, v. 64, p. 481–499.
- Stafleu, J., Everts, A.J.W., and Kenter, J.A.M., 1994, Seismic models of a prograding carbonate platform: Vercors, southeastern France: *Marine and Petroleum Geology*, v. 11, p. 514–517.
- Tipper, J.C., 1993, Do seismic reflections necessarily have chronostratigraphic significance?: *Geological Magazine*, v. 130, p. 47–55.
- Vail, P.R., Mitchum, R.M., and Thompson, S., III, 1977a, Cycles of relative changes of sea level, in Payton, C.E., ed., *Seismic stratigraphy—Applications to hydrocarbon exploration: American Association of Petroleum Geologists Memoir 26*, p. 83–97.
- Vail, P.R., Todd, A.G., and Sangree, J.B., 1977b, Chronostratigraphic significance of seismic reflections, in Payton, C.E., ed., *Seismic stratigraphy—Applications to hydrocarbon exploration: American Association of Petroleum Geologists Memoir 26*, p. 99–116.
- Westphal, H., 1998, Carbonate platform slopes—A record of changing conditions: Berlin, Springer-Verlag, *Lecture Notes in Earth Sciences*, v. 75, 197 p.
- Wilber, R.J., Milliman, J.D., and Halley, R.B., 1990, Accumulation of bank-top sediment in the western slope of Great Bahama Bank: Rapid progradation of a carbonate megabank: *Geology*, v. 18, p. 970–974.
- Wright, J.D., and Miller, K.G., 1993, Southern ocean influence on late Eocene to Miocene deep water circulation, in Kenneth, J.P., and Warnke, D.A., eds., *The Antarctic paleoenvironment: A perspective on global change: Antarctic Research Series*, v. 60, p. 1–25.

MANUSCRIPT RECEIVED BY THE SOCIETY OCTOBER 5, 1998
 REVISED MANUSCRIPT RECEIVED AUGUST 6, 1999
 MANUSCRIPT ACCEPTED AUGUST 30, 1999